

*Contrails*

WADD TECHNICAL REPORT 60-184

PART II

**EFFECT OF BASIC PHYSICAL PARAMETERS ON  
ENGINEERING PROPERTIES OF INTERMETALLIC COMPOUNDS**

✓  
J. H. WESTBROOK  
D. L. WOOD

GENERAL ELECTRIC RESEARCH LABORATORY

SEPTEMBER 1961  
✓

DIRECTORATE OF MATERIALS AND PROCESSES  
CONTRACT No. AF 33(616)-6144  
PROJECT No. 7350

*SA-10*  
AERONAUTICAL SYSTEMS DIVISION  
AIR FORCE SYSTEMS COMMAND  
UNITED STATES AIR FORCE  
WRIGHT-PATTERSON AIR FORCE BASE, OHIO

900 - December 1961 - 14-540 & 541

Approved for Public Release

# Contrails

## FOREWORD

This report was prepared by the General Electric Research Laboratory under USAF Contract No. AF33(616)-6144. This contract was initiated under Project No. 7350, "Refractory Inorganic Non-Metallic Materials" and Task No. 73500, "Ceramic and Cermet Materials Development." The work was administered under the direction of the Directorate of Materials and Processes, Deputy for Technology, Aeronautical Systems Division, with Lt T. E. Lippart acting as project engineer.

This report covers work conducted from December 1959 to December 1960.

The authors are greatly indebted to many members of the staff of the Metallurgy and Ceramics Research Department of the General Electric Research Laboratory for advice and assistance during the course of this investigation. W.A. Roman, Mrs M C Houle, and Miss A.M. Turkalo provided the metallographic and fractographic studies, L.C.Cook and D.C.Lord carried out the mechanical testing, A.J.Peat contributed to many of the experimental phases of the work. Beneficial discussions of the results were held with W.G. Johnston, R.L. Fleischer, and J.R. Low.

WADD TR 60-184 Part II

ABSTRACT

The tensile behavior of the CsCl structure compound AgMg are extensively documented in terms of strain, strain rate, temperature, grain size, composition, and metallurgical processing treatment. Three regimes of deformation behavior are observed: low temperatures, intermediate temperatures, and high temperatures. In each of these regimes different deformation processes operate. Specific findings have practical as well as scientific import. Certain exploratory studies on other intermetallics are also reported.

PUBLICATION REVIEW

This report has been reviewed and is approved.

FOR THE COMMANDER:

  
W. G. RAMKE

Chief, Ceramics and Graphite Branch  
Metals and Ceramics Laboratory  
Directorate of Materials and  
Processes

TABLE OF CONTENTS

	<u>Page</u>
I. INTRODUCTION . . . . .	1
II. EXPERIMENTAL PROCEDURES . . . . .	1
III. RESULTS FOR AgMg . . . . .	2
A. The Low-Temperature Region . . . . .	4
1. Observations on Flow Stress . . . . .	4
(a) Effects of Composition . . . . .	4
(b) Effects of Grain Size . . . . .	9
(c) Effects of Strain Rate . . . . .	10
(d) Effects of Strain . . . . .	10
2. Deformation Mechanism . . . . .	13
3. Ductility . . . . .	14
4. Fracture . . . . .	17
B. The Intermediate Temperature Region . . . . .	20
1. Manifestations of Dislocation Interaction with Solute Atoms (DISA) . . . . .	20
2. Analyses of Temperature and Rate Effects . . . . .	25
3. Grain Size Effects . . . . .	28
C. The High-Temperature Region . . . . .	29
1. Observations on Flow Stress . . . . .	29
(a) Effects of Temperature and Composition . . . . .	29
(b) Effects of Strain Rate . . . . .	31
(c) Effects of Grain Size . . . . .	33
(d) Effects of Strain . . . . .	33
2. Other Observations . . . . .	33

# Contrails

	<u>Page</u>
IV. DISCUSSION OF AgMg RESULTS . . . . .	33
A. The Low-Temperature Region . . . . .	33
1. Considerations of Flow Stress. . . . .	33
(a) Effects of Composition . . . . .	33
(b) Effects of Domains . . . . .	35
(c) Effects of Grain Size . . . . .	35
(d) Effects of Strain . . . . .	36
2. Considerations of Ductility . . . . .	36
(a) Effects of Prestrain. . . . .	36
(b) Effects of Composition . . . . .	39
3. Considerations of Fracture Mode . . . . .	40
B. The Intermediate Temperature Region. . . . .	40
1. Considerations of Flow Stress. . . . .	40
2. Recovery. . . . .	43
3. Mechanisms. . . . .	44
C. The High-Temperature Region . . . . .	44
V. STUDIES OF OTHER COMPOUNDS . . . . .	46
A. NiAl . . . . .	46
B. Bi <sub>2</sub> Tl. . . . .	47
C. TiAl . . . . .	47
D. LaPb <sub>3</sub> . . . . .	47
VI. SUMMARY AND CONCLUSIONS . . . . .	48
VII. RECOMMENDATIONS . . . . .	50
VIII. OTHER ACTIVITIES . . . . .	50
REFERENCES . . . . .	52
APPENDIX--SUMMARY OF TENSILE STRESS DATA . . . . .	57

# Contrails

## LIST OF ILLUSTRATIONS

<u>Figure</u>		<u>Page</u>
1	Photomicrograph of an AgMg wire in the as-extruded condition. 100X . . . . .	2
2	Typical load-elongation curves for the three regimes of deformation behavior: (1) low temperatures; (2) intermediate temperatures; (3) high temperatures. . . . .	3
3	Flow stress isotherms as a function of composition for AgMg, $\dot{\epsilon} = 0.5$ per cent $\text{min}^{-1}$ . . . . .	4
4	Flow stress as a double logarithmic function of defect concentration (from Fig. 3), showing a common slope for both excess Ag and excess Mg as well as for different grain sizes and temperatures . . . . .	6
5	Reduced stress $\sigma/\Delta^S$ as a function of temperature. . . . .	6
6	Effect of Various solutes on the lattice parameter of stoichiometric AgMg . . . . .	8
7	Relative change in flow stress of AgMg as a function of the relative change in lattice distortion resulting from additions of various solutes . . . . .	8
8	True stress-true strain curves showing values of the strain hardening exponent $m$ for AgMg compounds of different composition and grain size tested at various temperatures at a strain rate of $0.5$ per cent $\text{min}^{-1}$ . . . . .	11
9	Values of the strain hardening exponent, $m$ , as a function of composition for various temperatures and grain sizes . . . . .	11
10	Reduced stress $\sigma_{0.08}/\Delta^S$ as a function of temperature. . . . .	12
11	Strain hardening exponent, $m$ , plotted against the flow stress of various AgMg compounds tested at several temperatures, after annealing at $500^\circ\text{C}$ to an average grain diameter of $\sim 6.4 \times 10^{-3}$ cm . . . . .	13

List of Illustrations (contd)

<u>Figure</u>		<u>Page</u>
12	AgMg wires showing both the extent to which Ag-rich and Mg-rich compositions in the as-extruded condition can be bent by hand at room temperature, and the effect of high-temperature deformation on the room temperature ductility of Mg-rich wires . . . . .	15
13	Schematic representation of the effects of composition, strain rate, and temperature on the deformability of AgMg compounds . . . . .	17
14	Photomicrographs of fracture areas of AgMg tensile specimens strained at 0.5 per cent min <sup>-1</sup> . (a) 45.9 A/o Mg fractured at -196°C; (b) 49.0 A/o Mg fractured at RT; (c) 51.5 A/o Mg fractured at RT; (d) 51.5 A/o Mg fractured at 175°C. Specimens nickel plated. 100X . . . . .	18
15	Electronmicrograph of (211) cleavage in AgMg of near stoichiometric composition. 8400X . . . . .	19
16	Typical load-elongation curves obtained at several temperatures with a strain rate of 0.5 per cent min <sup>-1</sup> for various AgMg compounds using as specimens 0.040-inch-diameter wires with a 1-inch gage length . . . . .	21
17	Flow stress, increase in flow stress resulting from a 10X increase in strain rate, and increase in flow stress after 8 per cent elongation--shown for 43.9 A/o Mg as a function of temperature with a base strain rate of 0.5 per cent min <sup>-1</sup> . . . . .	23
18	Load-elongation curve obtained at 250°C for 51.2 A/o Mg with a specimen of 0.040-inch-diameter and 1-inch gage length, showing yield points and "inverse yielding" associated with changes in strain rate . . . . .	23
19	Typical load-elongation curves showing strain aging phenomenon: (a) initial loading; (b) immediate reloading; (c) reloading after aging . . . . .	24
20	Load-time relaxation curves (together with a load elongation curve) for 51.2 A/o Mg at a temperature of 270°C . . . . .	24

# Contrails

## List of Illustrations (contd)

<u>Figure</u>		<u>Page</u>
21	Flow stress as a function of the reciprocal of the absolute temperature for various AgMg compositions . . . . .	25
22	Variation of flow stress with strain rate at various temperatures for 51.2 A/o Mg . . . . .	26
23	Curves of flow stress vs strain rate (temperature compensated to a 250°C base) showing the best fit of points in the determination of energies involved in the flow process . . . . .	26
24	Microstructures of 54.3 A/o Mg tensile specimens tested at (a) 250°C; (b) 300°C; (c) 450°C. 1500X . . . . .	27
25	Flow stress of 51.2 A/o Mg as a function of the square root of the reciprocal of the grain diameter for various test temperatures . . . . .	28
26	Flow stress isotherms as a function of composition for AgMg (extended to higher temperatures from Fig. 3). $\dot{\epsilon} = 0.5$ per cent $\text{min}^{-1}$ . . . . .	29
27	Flow stress of both Ag-rich and Mg-rich compounds as a function of temperature. $\dot{\epsilon} = 0.5$ per cent $\text{min}^{-1}$ . . . . .	30
28	Effect of strain rate on the flow stress of 49.8 A/o Mg at several temperatures . . . . .	31
29	Curves of flow stress vs strain rate (temperature compensated to a 500°C base) showing the best fit of points in the determination of energies involved in the flow process . . . . .	32
30	Hardness and stress (at $\epsilon = 0.08$ ) at RT as a function of composition for material of grain size $\sim 1.7 \times 10^{-3}$ cm. (Each hardness value is the average of 10 indentations, each made in a different randomly selected grain.) . . . . .	35
31	Schematic representation of the rheotropic embrittlement phenomenon showing the effects of pre-strain, temperature, strain rate and stress state on ductility [after Rippling <sup>(52)</sup> ] . . . . .	38



# Contrails

## List of Illustrations (contd)

<u>Figure</u>		<u>Page</u>
32	Interrelated effects of temperature and strain rate on the ductility of a brittle material [after Magnusson and Baldwin <sup>(57)</sup> ] . . . . .	38
33	Activation energies for various high-temperature rate processes as a function of temperature . . . . .	45

# Contrails

## LIST OF TABLES

<u>Table</u>		<u>Page</u>
I	Stress ( $L/A_0$ ) at 0.2 Per Cent Offset at Various Temperatures for Specimens of Different Grain Sizes, Strained at a Rate of 0.5 Per Cent $\text{Min}^{-1}$ . Stress Given in 1000 psi . . . . .	9
II	A Comparison of Calculated and Observed Temperatures for the Incidence of Serrated Flow in AgMg Alloys . . . . .	43
III	Intended and Analyzed Compositions of AgMg Compounds . . . . .	57
IV	Stress ( $L/A_0$ ) at 0.2 Per Cent Offset for Various Temperatures and Strain Rates for Silver-rich Compounds; Given in 1000 psi for Material of Grain Diameter $\sim 1.7 \times 10^{-3}$ cm (as-extruded. . . . .	58
V	Stress ( $L/A_0$ ) at 0.2 Per Cent Offset for Various Temperatures and Strain Rates for Magnesium-rich Compounds; Given in 1000 psi for Material of Grain Diameter $\sim 1.7 \times 10^{-3}$ cm (as-extruded) . . . . .	58
VI	Stress ( $L/A_0$ ) at 0.2 Per Cent Offset for Various Temperatures and Strain Rates for Silver-rich Compounds; Given in 1000 psi for Material of Grain Diameter $\sim 2.8 \times 10^{-3}$ cm (annealed at $400^\circ\text{C}$ ) . . . . .	59
VII	Stress ( $L/A_0$ ) at 0.2 Per Cent Offset for Various Temperatures and Strain Rates for Magnesium-rich Compounds; Given in 1000 psi for Material of Grain Diameter $\sim 2.8 \times 10^{-3}$ cm (annealed at $400^\circ\text{C}$ ) . . . . .	60
VIII	Stress ( $L/A_0$ ) at 0.2 Per Cent Offset for Various Test Temperatures; Given in 1000 psi for Material of Grain Diameter $\sim 6.4 \times 10^{-3}$ cm (annealed at $500^\circ\text{C}$ ), Strained at a Rate of 0.5 Per Cent ( $\text{min}^{-1}$ ) . . . . .	61
XI	Stress ( $L/A_0$ ) at 8 Per Cent Elongation for Various Test Temperatures; Given in 1000 psi for Material of Grain Diameter $\sim 6.4 \times 10^{-3}$ cm (annealed at $500^\circ\text{C}$ ), Strained at a Rate of 0.5 Per Cent ( $\text{min}^{-1}$ ) . . . . .	62
X	Stress ( $L/A_0$ ) at Various Temperatures and Strain Rates; Given in 1000 psi for Material of Grain Diameter $\sim 10.2 \times 10^{-3}$ cm (annealed at $600^\circ\text{C}$ ) . . . . .	63

## EFFECT OF BASIC PHYSICAL PARAMETERS ON ENGINEERING PROPERTIES OF INTERMETALLIC COMPOUNDS

J. H. Westbrook and D. L. Wood

### I. INTRODUCTION

Of all the material groups of potential interest as high-temperature structural materials, the intermetallics have been the least studied, particularly with respect to their mechanical behavior. Moreover, the application and processing of intermetallics for uses which exploit their often unique physical properties have been impeded by a lack of understanding of their mechanical properties.

Previous work in this area\* has been largely exploratory, aimed on the one hand at the direct empirical development of materials of engineering utility, and on the other at identification of the important parameters affecting the mechanical behavior of intermetallics. As a consequence, there has not been available, heretofore--for any intermetallic--data, sufficient in extent or precision to provide an adequate phenomenological description of the effects of metallurgical variables on deformation behavior. Such documentation is prerequisite to intelligent application or processing design and is also necessary for testing present and future theoretical analyses of mechanical behavior. It was therefore an objective of the present investigation to document the deformation behavior of a simple ordered intermetallic over as wide a range as possible of all the usual metallurgical variables.

### II. EXPERIMENTAL PROCEDURES

Initial steps in such a program are obviously the selection of an appropriate compound or compounds, the development of a satisfactory process for specimen preparation and the adoption of a testing technique. These matters as well as certain preliminary results have already been described elsewhere in some detail.<sup>(2-4)</sup> This report is concerned primarily with the first extensive phase of the program which has been completed, namely a study of the tensile behavior of extruded polycrystalline wires of AgMg, a compound having the CsCl structure. Some preliminary results on some other simple intermetallics are also recorded.

---

\*For a recent review see Westbrook.<sup>(1)</sup>

Manuscript released for publication 31 March 1961 as a WADD Technical Report.

### III. RESULTS FOR AgMg

For the most part, the experimental results consist of tensile flow curves obtained on single-phase polycrystalline wires, of the structure shown in Fig. 1, using various combinations of temperature, strain rate, composition, grain size, and heat treatment. In numerous instances several tests were run to ensure reproducibility of the results. These tests showed mean deviations in flow stress of less than 2 per cent at room temperature. The tensile data obtained are summarized in the Appendix.\*

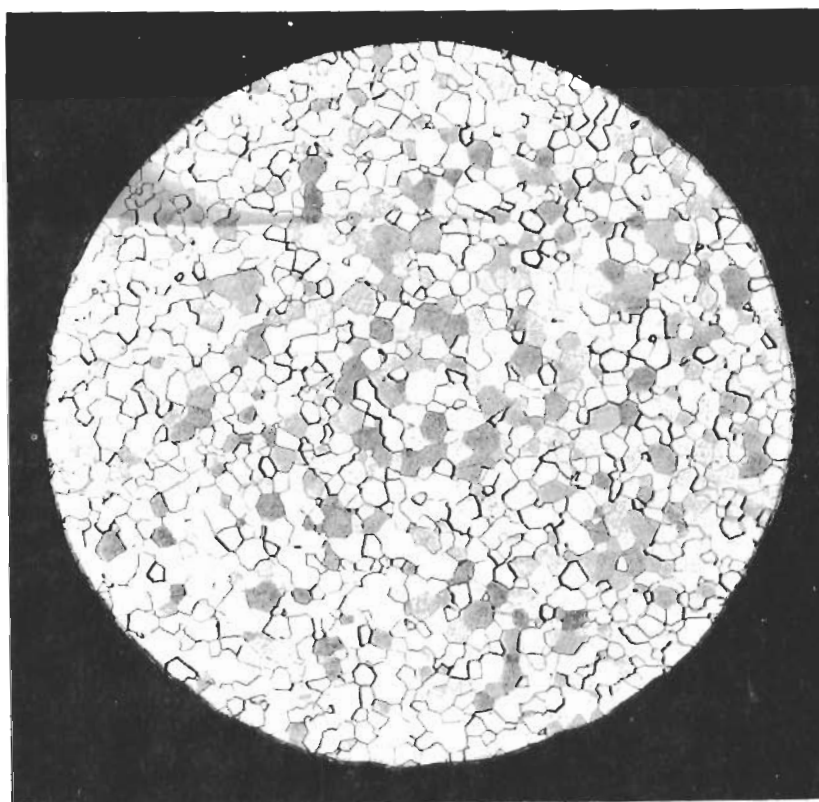


Fig. 1 Photomicrograph of an AgMg wire in the as-extruded condition. 100X

---

\*Tensile stress data are reported in this report as engineering stresses (load/original cross-sectional area) unless otherwise noted. This procedure is considered adequate for small uniform elongations.

Analyses of the tensile data together with the results of certain auxiliary experiments permit distinction of three regimes of deformation behavior:

- (1) Low temperatures and moderate strain rates where deformation is primarily by slip.
- (2) Intermediate temperatures and low to moderate strain rates where deformation behavior is dominated by dislocation interactions with solute atoms--DISA phenomena.\*
- (3) High temperatures and low strain rates where deformation is primarily by diffusion controlled processes.

The load-elongation curves for these three regimes are quite distinctive as can be seen by the typical examples shown in Fig. 2.

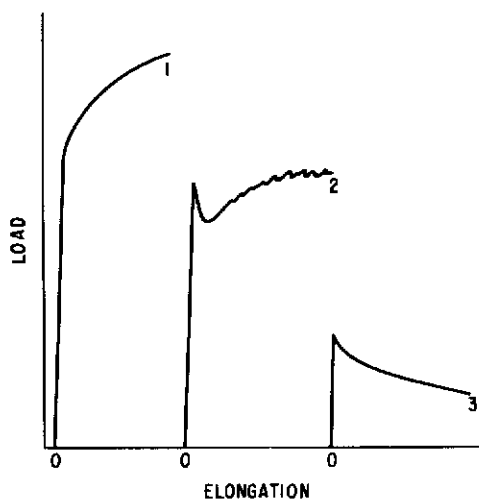


Fig. 2 Typical load-elongation curves for the three regimes of deformation behavior: (1) low temperatures; (2) intermediate temperatures; (3) high temperatures.

---

\*The term "DISA phenomena" is used here collectively for all possible interactions of dislocations with solute atoms tending to segregate to the vicinity of the dislocation. For the most part the situation of static dislocations and moving solutes [whether the appropriate model is one of unpinning<sup>(5, 6)</sup> or of dislocation multiplication<sup>(7)</sup>] is not distinguished from the dynamic case of moving dislocations and moving solute atoms [the only detailed model of which<sup>(8)</sup> seems quite inadequate for the general case].

## A. The Low-Temperature Region

### 1. Observations on Flow Stresses

(a) Effects of Composition. The most prominent characteristic exhibited by specimens tested up to about 150°C is the marked influence of composition (within the single phase region) on the tensile properties. One of these effects can be observed from Fig. 3 which shows isotherms of the 0.2 per cent offset flow stress as a function of composition. Sharp minima occur at the stoichiometric composition and persist over an extensive temperature range. These minima correspond to those previously found by Westbrook in indentation hardness studies in AgMg<sup>(9)</sup> and by others in a variety of other intermetallics (for a review see Ref. 1). Such minima were attributed by Westbrook to the presence in off-stoichiometric compositions of point defects which impede slip. Data of the type shown

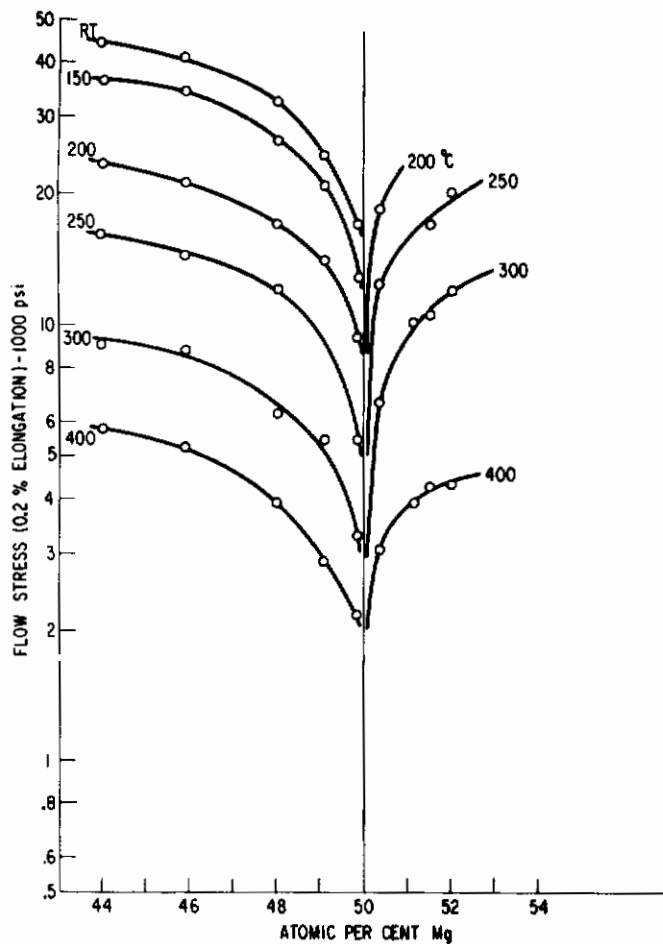


Fig. 3 Flow stress isotherms as a function of composition for AgMg,  $\dot{\epsilon} = 0.5$  per cent  $\text{min}^{-1}$ .

in Fig. 3 may be more readily assessed from Fig. 4 which plots the logarithm of the flow stress against the logarithm of the defect concentration for some representative isotherms. Note that straight parallel lines are obtained for several sets of specimens: silver-rich compositions, magnesium-rich compositions, and samples of different grain sizes. Extrapolation of the lower temperature isotherms to low defect concentrations\* permits determination of a flow stress at an effective "stoichiometric" composition; such a determination is difficult with the sharp curvatures found in Fig. 3.

If lattice defects, whose concentration is measured by deviation from stoichiometric composition, are predominantly responsible for the flow stress level in the low-temperature range, then it might be expected that the stress-temperature data would be simplified by using a reduced stress  $\sigma/\Delta^s$ , where  $\Delta$  is the deviation from stoichiometry and  $s$  is the slope of the lines in Fig. 4. Treatment of the data from Fig. 3 by this method results in the curves shown in Fig. 5. It can now be seen, as is apparent but less clear in Figs. 3 and 4, that excess magnesium defects are a more potent impediment to flow than are excess silver defects in the temperature region below about 400°C. The merging of the two separate branches into a common curve at higher temperatures might be taken as a difference in the temperature dependence of the defect hardening behavior of the two types of atoms. However, this appearance may merely be a result of slight differences in response to DISA phenomena which become prominent in the intermediate temperature range.

By taking the simplest view that solid solution strengthening is primarily due to lattice strain,<sup>(10)</sup> and assuming that excess magnesium and excess silver atoms affect the lattice only through the lattice strain they impart, two predictions can be made. First, the slope of the lines for magnesium-rich compositions should be equal to that for silver-rich compositions, since it is to be presumed that, to a first approximation, lattice strain is proportional to defect concentration of either type. This prediction may be confirmed by inspection of Fig. 4. Secondly, the relative change in flow stress should be proportional to the relative change in lattice distortion.

To check the latter prediction, the strain imparted by both magnesium and silver excesses can be determined from lattice parameter measurements. Two sets of parameter data are available: one determined by Ageev and Kuznetsov<sup>(11)</sup> and one obtained in an auxiliary study<sup>(12)</sup> during the present investigation. These parameter results are in substantial agreement and they, together with density<sup>(12)</sup> and x-ray experiments,<sup>(11)</sup> show the defects to be substitutional on both sides of stoichiometry. Magnesium atoms substituting for

---

\*A concentration of 0.01 A/o Ag was arbitrarily chosen.

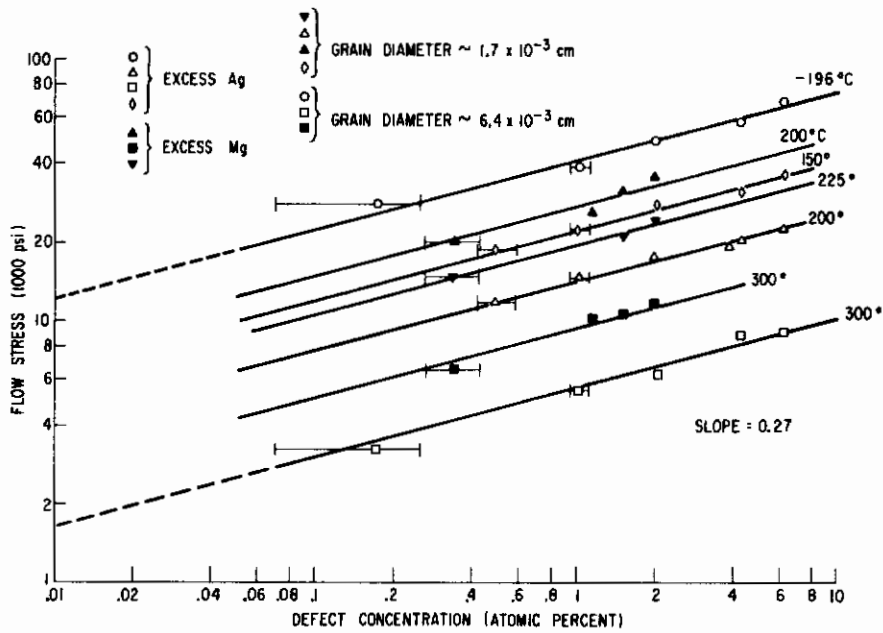


Fig. 4 Flow stress as a double logarithmic function of defect concentration (from Fig. 3), showing a common slope for both excess Ag and excess Mg as well as for different grain sizes and temperatures.

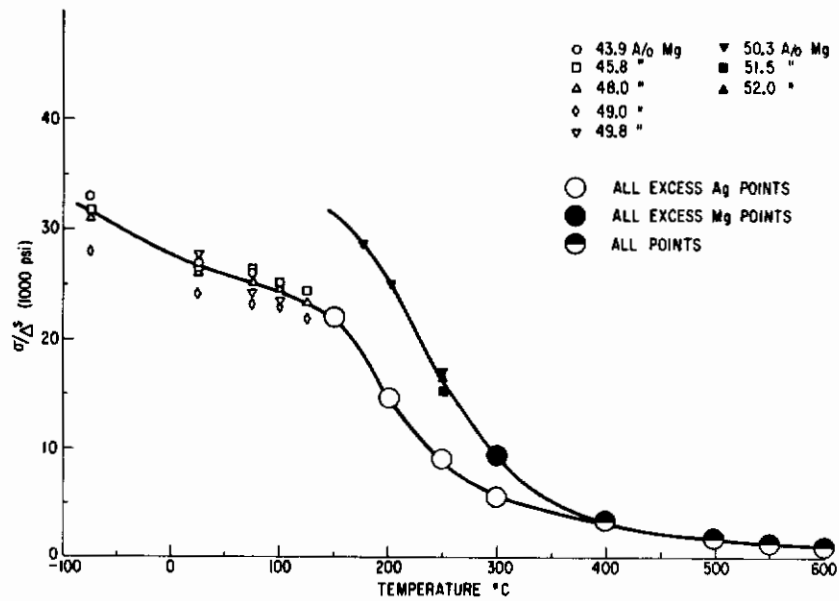


Fig. 5 Reduced stress  $\sigma/\Delta^S$  as a function of temperature.



silver expand the lattice and silver atoms substituting for magnesium contract it; the distortion resulting from unit magnesium excess is greater than that for unit silver excess. Qualitative agreement with the results of Fig. 5 is thus indicated.

Further confirmation was sought by examining the effects of ternary solid solution additions. Three solutes were selected: zinc, tin, and lead. Zinc is a relatively small atom and would be expected to contract the lattice of the compound; tin and lead are large atoms and would be expected to expand the lattice. Ternary alloys, made by adding 1 at. per cent of solute element to a stoichiometric AgMg base, were processed to 0.040-inch wire in the same manner as was used for the binary alloys. Successful results were obtained except for the lead containing material which proved to be hot short (a result due at least in part to the presence of Pb-rich second phase). Tensile tests and lattice parameter measurements were made on both the tin and the zinc containing samples after metallographic examination verified their single-phase constitution. Lattice parameters were measured on filed powders which had been strain relieved in argon at 400°C. The results of the parameter measurements on the ternary alloys are shown in Fig. 6 which also reproduces results obtained for the binary compositions. It was found that tin additions expand the lattice of AgMg to almost the same degree as do excess magnesium atoms, while zinc additions contract it to only a slightly greater degree than do excess silver atoms.

A quantitative assessment of the correlation between defect strengthening and lattice strain can now be made in Fig. 7 in which the relative change in flow stress per atom per cent defect is plotted against the relative change in lattice distortion per atom per cent defect. Points are plotted for both types of off-stoichiometry binary compounds and for the two ternary alloys. Since tensile data could not be obtained at room temperature for all compositions and since it was inconvenient to make parametric measurements at high temperature, comparison must be made of 100° and 200°C tensile data with room temperature lattice strain measurements. This procedure probably does not involve much error since the elastic moduli would be expected to vary only slightly over this temperature range. If the presumption is correct that defect hardening is primarily due to lattice strain, then a line through the points of Fig. 7 should extrapolate through the origin. Since a line of best fit did not pass exactly through the origin, the line drawn is that which represents the best line passing through the group of points and through the origin. The agreement with prediction, however, is probably within the precision of the measurements. The absence of pronounced valence or "chemical" effects is indicated by the approximately equivalent behavior of mono-, di-, and tetra-valent solutes.

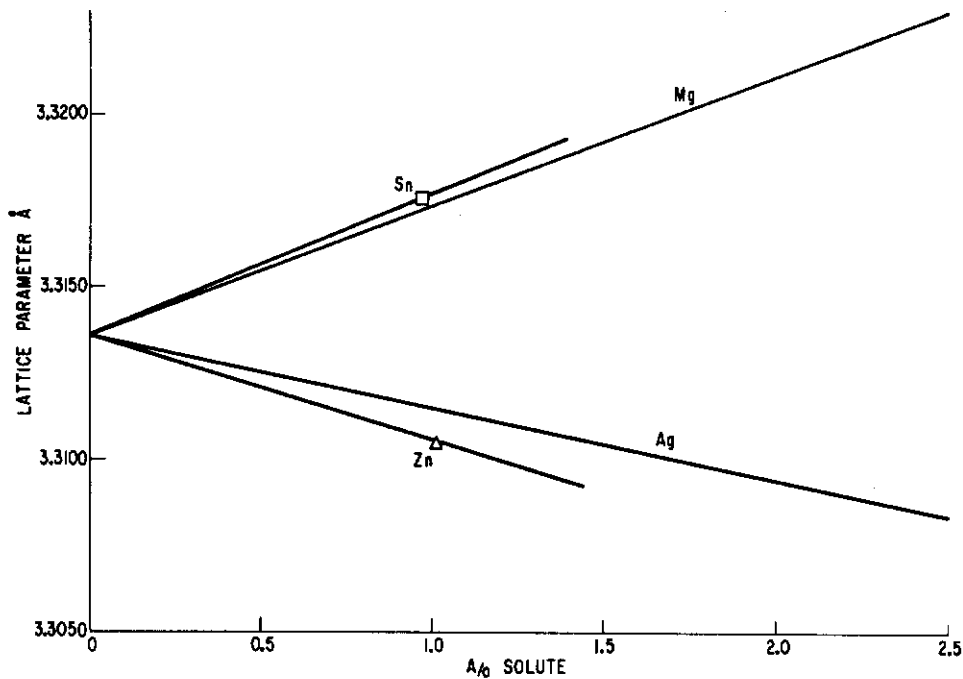


Fig. 6 Effect of various solutes on the lattice parameter of stoichiometric AgMg.

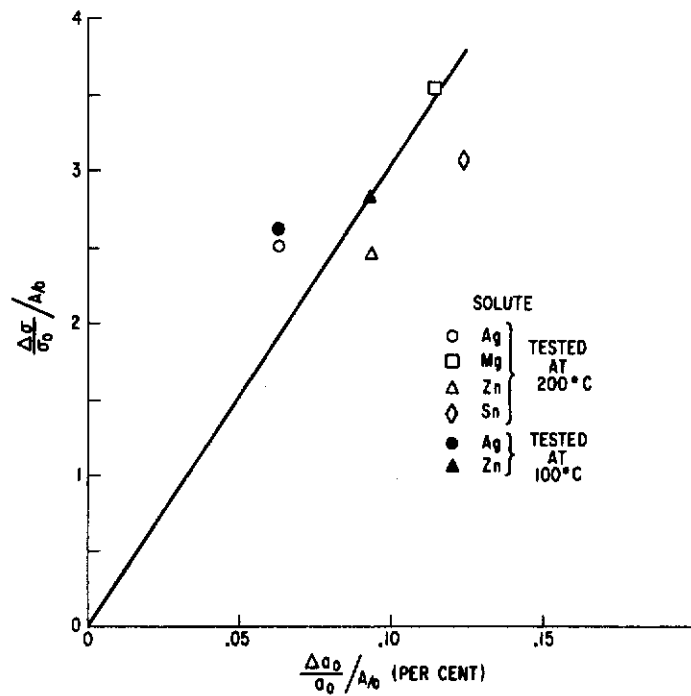


Fig. 7 Relative change in flow stress of AgMg as a function of the relative change in lattice distortion resulting from additions of various solutes.

(b) Effects of Grain Size. Studies of the effect of grain size on the flow stress were made using as specimens material in the as-extruded condition (grain diameter  $\sim 1.7 \times 10^{-3}$  cm), material annealed at  $400^{\circ}\text{C}$  (grain diameter  $\sim 2.8 \times 10^{-3}$  cm), and material annealed at  $500^{\circ}\text{C}$  (grain diameter  $\sim 6.4 \times 10^{-3}$  cm). It was observed, as is shown in Table I, that although the flow stress of specimens of the largest grain size (annealed at  $500^{\circ}\text{C}$ ) was lower than that of specimens of intermediate grain size (annealed at  $400^{\circ}\text{C}$ ), as is normal for pure metals, the flow stress values for fine grained (as-extruded) specimens were considerably lower than would be expected in normal behavior.

Since both the specimens of large and intermediate grain size had been annealed following extrusion, while the specimens of fine grain size were tested in the as-extruded condition, it was felt that this lack of annealing might in some way be responsible for the relatively low values of flow stress observed in the as-extruded material. Extruded specimens, therefore, were annealed at a temperature of  $250^{\circ}\text{C}$  at which no grain growth occurs, and the flow stress measured. It was found that although the flow stress of these annealed specimens was consistently somewhat higher than that of as-extruded material, the values were still considerably lower than that required to fulfill the usual grain size relationship.

TABLE I

Stress ( $L/A_0$ ) at 0.2 Per Cent Offset at Various Temperatures  
for Specimens of Different Grain Sizes, Strained at a Rate  
of 0.5 Per Cent  $\text{Min}^{-1}$ . Stress Given in 1000 psi

Test Temp ( $^{\circ}\text{C}$ )	43.9 A/o Mg			49.0 A/o Mg		
	As- extruded (a)	Ann. $400^{\circ}\text{C}$ (b)	Ann. $500^{\circ}\text{C}$ (c)	As- extruded (a)	Ann. $400^{\circ}\text{C}$ (b)	Ann. $500^{\circ}\text{C}$ (c)
25	45.6	48.0	44.5	28.8	21.2	24.3
100	40.8	46.0	41.7	26.7	25.6	23.2
150	37.1	38.4	36.7	22.2	23.2	20.9
200	22.8	24.0	23.5	14.8	14.1	14.0

(a) Grain diameter =  $1.7 \times 10^{-3}$  cm

(b) Grain diameter =  $2.8 \times 10^{-3}$  cm

(c) Grain diameter =  $6.4 \times 10^{-3}$  cm

(c) Effects of Strain Rate. The effects of strain rate on the flow stress were observed to be quite small in the lower part of this temperature range--so small, in fact, that it was difficult to obtain quantitative measurements from tests on different specimens. Resort was made, therefore, to a "rate-change" test in which a selected slow rate was maintained through yielding to a small value of plastic strain where the rate was changed by a factor of ten and the test continued. Rate sensitivity,  $n$ , as defined by the ratio of the change in the logarithm of the flow stress to the change in the logarithm of the strain rate, was readily determined from the autographic record of the testing machine. Values for  $n$  of the order of 0.01 were found for silver-rich specimens. Coarse grained specimens and tests at temperatures near the upper end of this range ( $\sim 150^\circ\text{C}$ ) gave slightly higher values. These observations are all in accord with the behavior of pure metals.

(d) Effects of Strain. The foregoing discussion treated only the initial flow stress (0.2 per cent offset). Consideration of the effects of strain brings forth other points of interest. Analyses were first made to see if the data conformed to the empirical relation

$$\sigma = K\epsilon^m \quad (1)$$

which frequently well approximates the behavior of metals. In this expression  $\sigma$  is the true stress,  $\epsilon$  is the true strain, and  $K$  and  $m$  are constants. Data from the autographic load-elongation charts were reduced for this purpose by means of the usual relations:

$$\sigma = (P/A_0)(1+e) \text{ and } \epsilon = \ln(1+e)$$

where  $P$  = applied load,  $A_0$  = original cross-sectional area, and  $e$  = elongation. Examples of conformance of the present data to Eq. (1) are shown in Fig. 8. Values for  $m$  derived from curves as in Fig. 8 at various temperatures, compositions and grain sizes are shown in Fig. 9. The trends in  $m$  with temperature and grain size as well as the order of the numerical values for the stoichiometric composition are comparable with behavior common for metals. For example, silver<sup>(13)</sup> at an equivalent homologous temperature has an  $m = 0.5$ ; vanadium,<sup>(14)</sup> 0.1; molybdenum,<sup>(15)</sup> 0.25; tantalum,<sup>(16)</sup> 0.2; and tungsten,<sup>(17)</sup>  $> 0.4$ . The effects of the state of order on the strain hardening capacity are in agreement with those which have been seen in a variety of intermetallic studies dating back to the classic observations of Sachs and Weerts.<sup>(18)</sup>

The effects of solute concentration (i. e., excess Ag or Mg) on flow stress at moderate strains ( $\sim 0.08$ ) were found to be generally the same as had been found for the 0.2 per cent offset flow stress (see Fig. 4) except at low temperatures ( $< 200^\circ\text{C}$ ) where the exponential factor  $s$  in the expression  $\sigma = K\Delta^s$  is appreciably lower. For example, at room temperature and a strain of 0.08,  $s \approx 0.13$  but at  $200^\circ\text{C}$   $s \approx 0.27$  just as for the 0.2 per cent offset stress. This result appears to

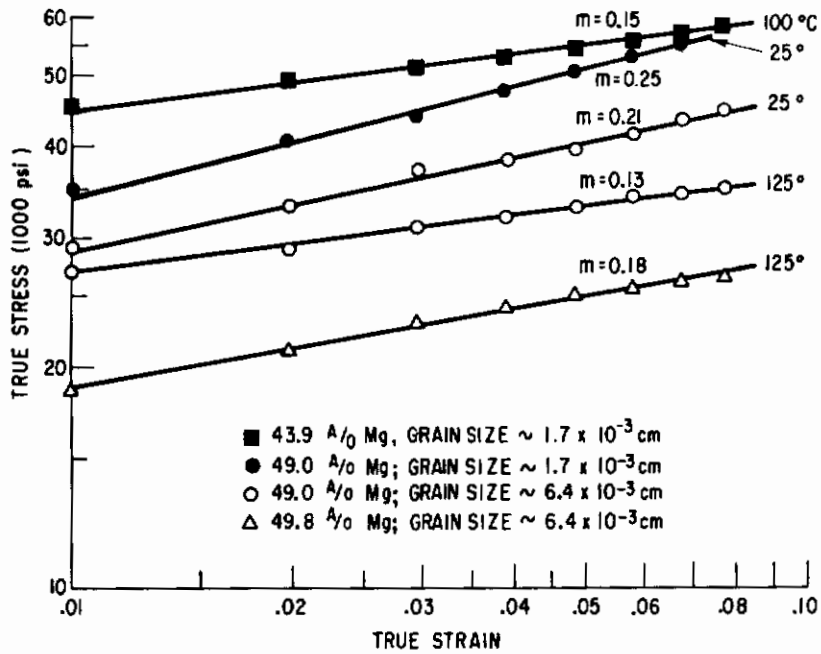


Fig. 8 True stress-true strain curves showing values of the strain hardening exponent  $m$  for AgMg compounds of different composition and grain size tested at various temperatures at a strain rate of 0.5 per cent  $\text{min}^{-1}$ .

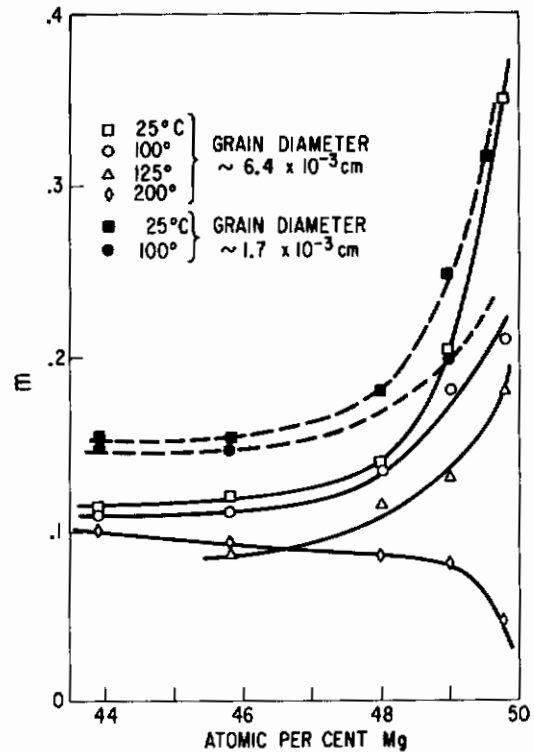


Fig. 9 Values of the strain hardening exponent,  $m$ , as a function of composition for various temperatures and grain sizes.

be a reflection of the dependence of strain hardening capacity on composition as shown in Fig. 9. If reduced stresses,  $\sigma_{0.08}/\Delta^s$ , are plotted against temperature as was done in Fig. 5, but now using a value for  $s$  which is appropriate to each temperature, a bifurcate curve is obtained which is exactly analogous to that of Fig. 5 and which has comparable scatter of the data points. Figure 10 shows  $\sigma_{0.08}/\Delta^s$  with  $s$  taken as 0.27 at all temperatures to illustrate the increased and systematic spread in the reduced stress values at low temperatures unless the appropriate  $s$  values are used. The complementary effects of defect structure on 0.2 per cent offset flow stress and strain hardening suggest a relation of the sort observed by Hollomon<sup>(19)</sup> in tensile tests on a series of steels and on  $\alpha$  brasses:

$$\log m = K - K' \log \sigma \quad (2)$$

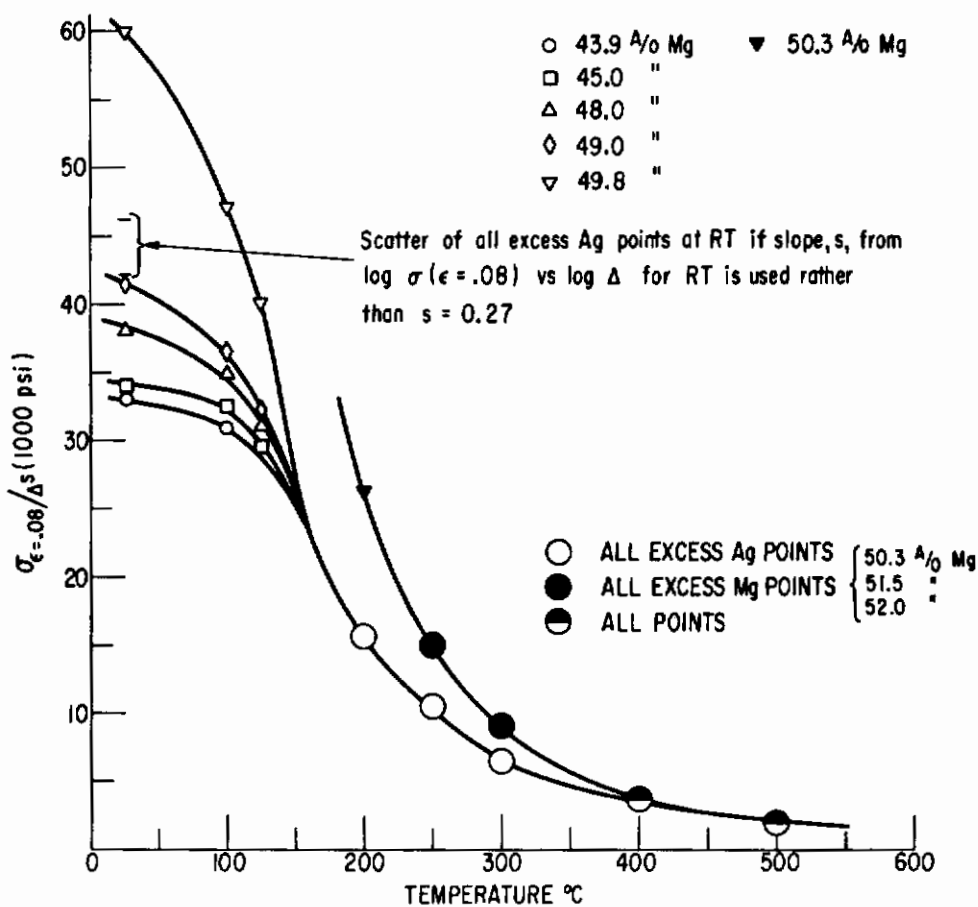


Fig. 10 Reduced stress  $\sigma_{0.08}/\Delta^s$  as a function of temperature.

where K and K' are constants depending on the temperature and the composition of the material tested. Such an analysis of some of the present data is shown in Fig. 11.

More limited data were obtained for the effects of strain in ternary alloys. Only for the zinc alloy could flow curves be extended as high as 0.08 strain. The  $\sigma = K \epsilon^m$  relationship was again obeyed in the low-temperature region. Values of m were significantly higher and temperature dependence of m lower than for silver-rich binary alloys of equivalent 0.2 per cent offset flow stress.

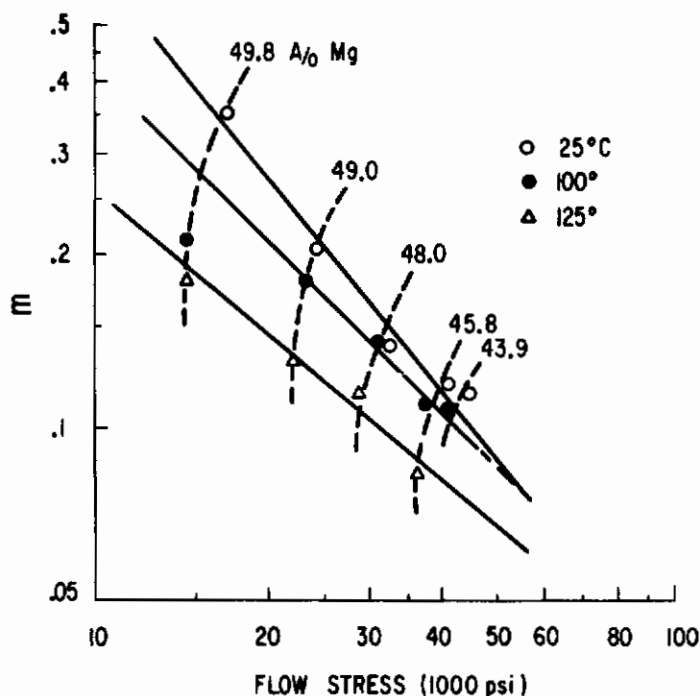


Fig. 11 Strain hardening exponent, m, plotted against the flow stress of various AgMg compounds tested at several temperatures, after annealing at 500°C to an average grain diameter of  $\sim 6.4 \times 10^{-3}$  cm.

## 2. Deformation Mechanism

The observations thus far discussed conform in the main to behaviors exhibited by normal metals, solid solution strengthened and deforming by slip. Direct evidence of the deformation mechanism was sought by deforming single crystals prepared by gradient freezing in graphite molds. Although typical slip markings were evidenced, detailed crystallographic analyses were not carried out on such specimens because of the difficulty of producing a large number of single-crystal specimens of appropriate size and controlled orientation and composition.

Instead, application was made of indentation deformation, thus permitting the use of coarse-grained polycrystalline samples which were already available. Slip traces about Vickers hardness indentations in x-ray oriented grains were analyzed stereographically.

A detailed report of this study will be made at a later time, but the preliminary conclusion may be stated. Slip was found to occur on the  $\{321\}$ ,  $\{211\}$ , and  $\{110\}$  planes. The slip direction is almost certainly  $\langle 111 \rangle$  although a direct unambiguous determination is not possible in a single surface experiment. The reasons for claiming a  $\langle 111 \rangle$  direction are: it is the direction previously reported by Rachinger and Cottrell;<sup>(20)</sup> it is a close-packed direction; planes showing traces about a given indentation belong to common  $\langle 111 \rangle$  zones; and coupling of the appropriate  $[111]$  direction with the observed slip plane leads to reasonable movement of material from the center of the indentation toward the outside. No significant effects of temperature or composition on the slip system were observed although slip lines tend toward pencil glide with increasing temperature and become unresolvable with ordinary techniques at  $400^{\circ}\text{C}$ . The present result differs from that of Rachinger and Cottrell<sup>(20)</sup> in the finding of  $\{211\}$  and  $\{110\}$  as well as  $\{321\}$ . It is more nearly in accord with Ardley and Cottrell<sup>(21)</sup> who found  $\{321\}$ ,  $\{211\}$  and  $\{110\}$  slip in  $\beta$  brass although in their case, choice of slip plane was apparently affected by temperature.

### 3. Ductility

A general shortcoming of all intermetallics in most practical uses is their lack of ductility at ordinary temperatures. Although almost all intermetallics become ductile at high homologous temperatures, very few show any sensible ductility below about 0.4 of their absolute melting temperature. One of the ultimate objectives, therefore, of an investigation of the mechanical behavior of intermetallics is to gain sufficient insight into the nature of this low-temperature brittleness to devise a solution to the brittleness problem, if such be possible. In the present investigation a qualitative study was made of the effects of composition, strain rate, temperature, and grain size on the low-temperature ductility.

Although it appears impossible to impart any macro-scale plastic deformation to as-cast material, certain processing techniques as well as certain conditions of prior high-temperature deformation were found to confer substantial amounts of ductility when subsequently examined at ordinary temperatures. No measurements of elongation to fracture were made on cast material due to extreme difficulty in the preparation of satisfactory test specimens from as-cast material. The absence of ductility at room temperature, however, is evidenced by qualitative observations. Cast ingots, for example, can be shattered easily by striking with a hammer. Small pieces of cast material, slowly squeezed in a vise, fracture with no evidence of having undergone any plastic deformation.



The processing of cast ingots by two stage extrusion at  $0.7 T_{mp}$  to final specimen shape (0.040-inch-diameter wire) was found to enhance considerably the room temperature ductility of all silver-rich alloys while no apparent improvement was found at that temperature for any magnesium-rich alloy. Figure 12 shows, for example, that a very slightly silver-rich wire in the as-extruded condition can be readily bent at room temperature, but extruded wires containing only as much as 0.3 A/o excess magnesium exhibit no room temperature ductility. Although the processing by extrusion did not observably increase the room temperature ductility of the magnesium-rich alloys, it can be seen also from Fig. 12 that slow tensile deformation in an appropriate temperature region can increase considerably the room temperature ductility of magnesium-rich alloys.

The ductility of extruded silver-rich material was not removed by annealing for an hour at  $600^{\circ}\text{C}$  although the ductility of the coarse-grained material thus annealed was lower than that of the fine-grained extruded material. This result is probably mostly an effect of grain size, for it was found generally that specimens of small grain size exhibited considerably more ductility than did specimens of large grain size. (Statements such as the last one are based not so much on quantitative measurements of elongation to fracture--which were erratic and poorly reproducible--as on the ability of fine-grained material to flow at faster strain rates and lower temperatures than was possible for coarse-grained material.) On the other hand, magnesium-rich wires, enductiled by slow deformation in a tensile test, regained their severe brittleness upon short-time annealing at temperatures around  $250^{\circ}\text{C}$  or by long-time annealing (weeks) at room temperature.

Further experiments were carried out in the hope of clarifying the nature of the enductilement produced in silver-rich wires by extrusion. Extruded wires of several silver-rich compositions were successfully cold-rolled from 0.040-inch diameter to strip 0.020 inch thick. Annealing of these strips at a temperature of about  $300^{\circ}\text{C}$  resulted in complete recrystallization to a grain size comparable to

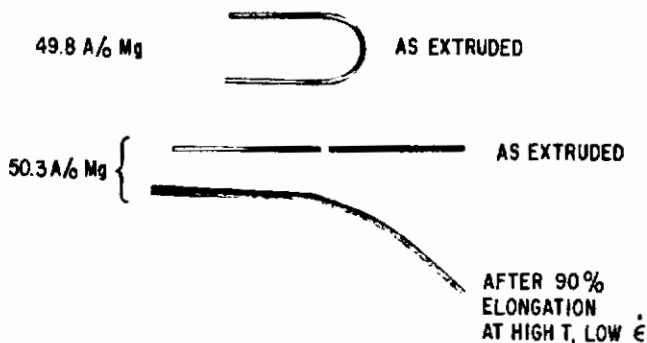


Fig. 12 AgMg wires showing both the extent to which Ag-rich and Mg-rich compositions in the as-extruded condition can be bent by hand at room temperature, and the effect of high-temperature deformation on the room temperature ductility of Mg-rich wires.

# Contrails

that in the as-extruded wires. It was found that the recrystallized strips no longer had the ductile characteristics of the extruded wires, but rather had a degree of brittleness comparable to the extruded magnesium-rich wires.

One possible explanation of such an observation is that the ductility of as-extruded silver-rich wires is due to the presence of a texture in the wires, and that the removal of this texture by recrystallization is responsible for the return of brittleness. A very slight degree of texture, with [110] as the fiber axis, is observed in extruded wires of both silver-rich and magnesium-rich compositions. Since texture studies are difficult on wire specimens, it was hoped that thin sheet formed by extrusion would lend itself to a study of the effect of texture on ductility. Careful processing enabled the extrusion of silver-rich material to strip 0.25 x 0.005 inch. Unfortunately, it was found that such extruded strip was completely brittle and therefore could not be used for the intended study. The negative result, however, is another indication of the critical relationship between the conditions of prior hot work and subsequent cold deformability. Experimental work on sheet extrusion textures has been temporarily abandoned.

While at ordinary and moderately elevated temperatures a rather sharp boundary appears to exist at the stoichiometric composition between the ductility of silver-rich and magnesium-rich compounds, the ductility is observed qualitatively to decrease with increasing magnesium content in compounds on both sides of stoichiometry. This effect can be seen in silver-rich compounds by the extent to which extruded wires can be bent at room temperature, and in the magnesium-rich compounds by the lowest possible tensile testing temperature for a given strain rate.

The ductility of all compositions was found to be quite sensitive to strain rate. However, even with the slowest strain rate available (0.02 per cent  $\text{min}^{-1}$ ), it was found impossible to impart any substantial plastic elongation to magnesium-rich compounds (even those close to stoichiometry) at temperatures below about 175°C. It will be noted, therefore, throughout this report, that even though stress data are reported for silver-rich compounds at temperatures as low as -196°C, no data are reported for magnesium-rich compounds below about 175°C ( $\sim 0.4 T_{\text{mp}}$ ).

The strain rate normally employed in the tensile tests reported here was 0.5 per cent  $\text{min}^{-1}$ . It was possible to initiate flow in silver-rich compounds at this strain rate at temperatures as low as -196°C, but in magnesium-rich compounds at temperatures only as low as 175° to 200°C. It was observed, however, that after plastic flow had been successfully initiated at a slow strain rate, the specimen could be made to flow at strain rates as much as 100 times faster than the initial strain rate.

Strained in tension at  $-196^{\circ}\text{C}$  at a rate of  $0.5$  per cent  $\text{min}^{-1}$ , silver-rich compounds were found to fracture after about 1 per cent elongation, while at room temperature the elongation to fracture was of the order of 10 to 20 per cent. Elongations of the order of 100 per cent were obtained at temperatures around  $200^{\circ}\text{C}$  for silver-rich compounds, while for magnesium-rich compounds elongations of this magnitude could only be obtained at temperatures at or above about  $250^{\circ}\text{C}$ . These relationships are shown graphically in Fig. 13.

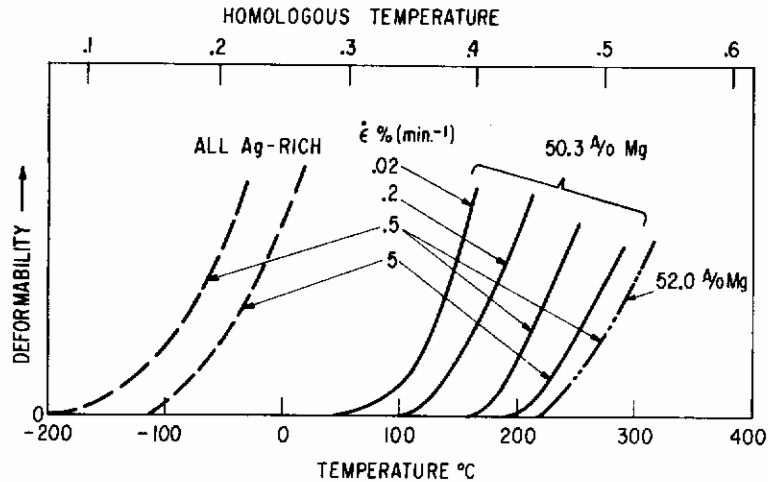


Fig. 13 Schematic representation of the effects of composition, strain rate, and temperature on the deformability of AgMg compounds.

#### 4. Fracture

Fracture in this temperature range was predominantly intergranular for all ordinary strain rates, even at the lowest temperatures, and for both silver-rich and magnesium-rich samples. Representative tensile fractures are shown in Fig. 14.

Impact of single crystals and coarse-grained specimens, on the other hand, produced extensive transgranular cleavage failure. Laue back reflection analyses of cleavage faces revealed  $\{211\}$  planes exclusively. This plane is not a common cleavage plane for body-centered cubic structures although it is found both as a twinning plane and a slip plane. (22)

Some cleavage surfaces were studied by electron fractography using techniques similar to those employed by Guard and Turkalo. (23) A typical example is shown in Fig. 15. Many features of the fractograph in Fig. 15 as well as in

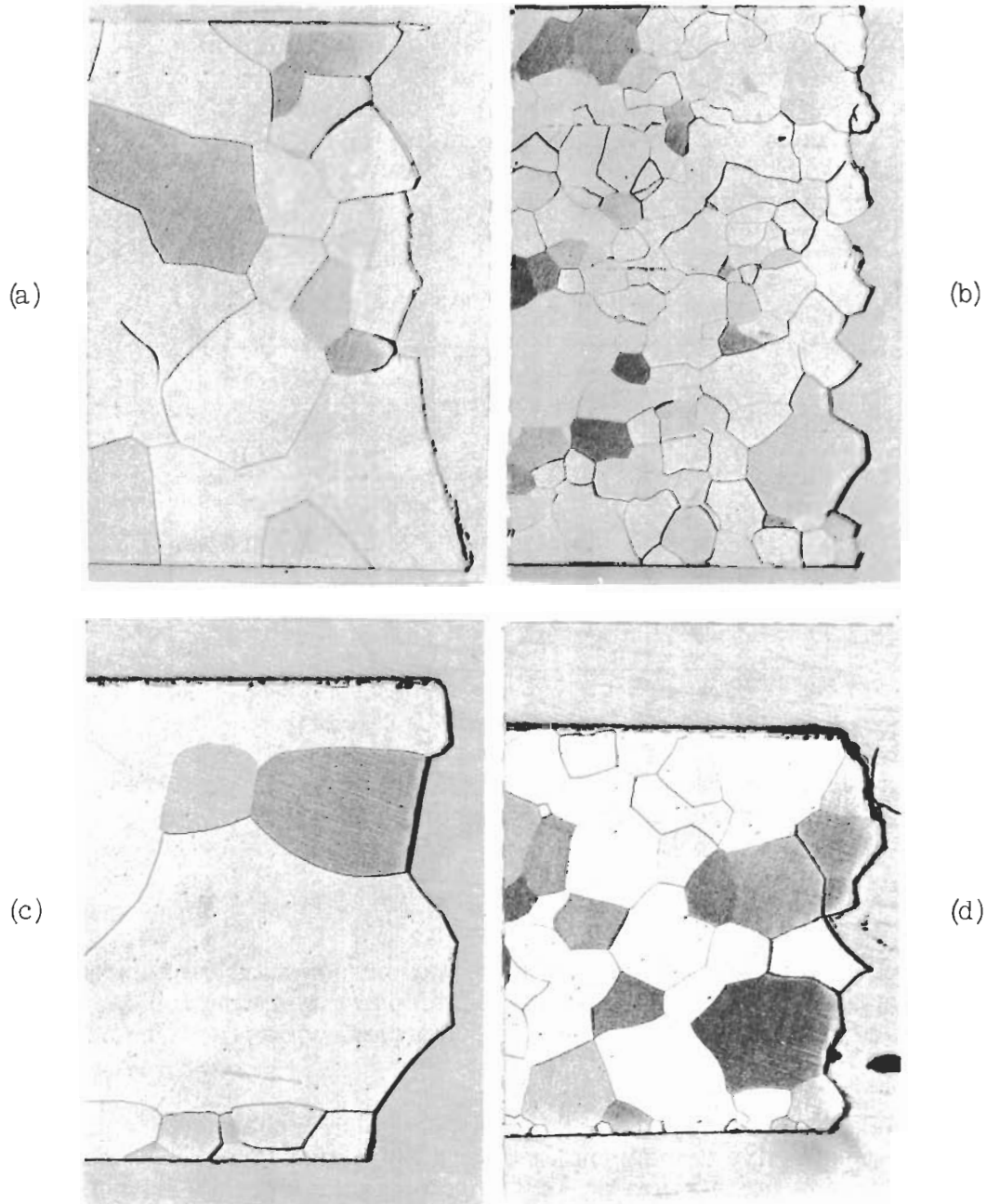


Fig. 14 Photomicrographs of fracture areas of AgMg tensile specimens strained at 0.5 per cent  $\text{min}^{-1}$ . (a) 45.9 A/o Mg fractured at  $-196^{\circ}\text{C}$ ; (b) 49.0 A/o Mg fractured at RT; (c) 51.5 A/o Mg fractured at RT; (d) 51.5 A/o Mg fractured at  $175^{\circ}\text{C}$ . Specimens nickel plated. 100X

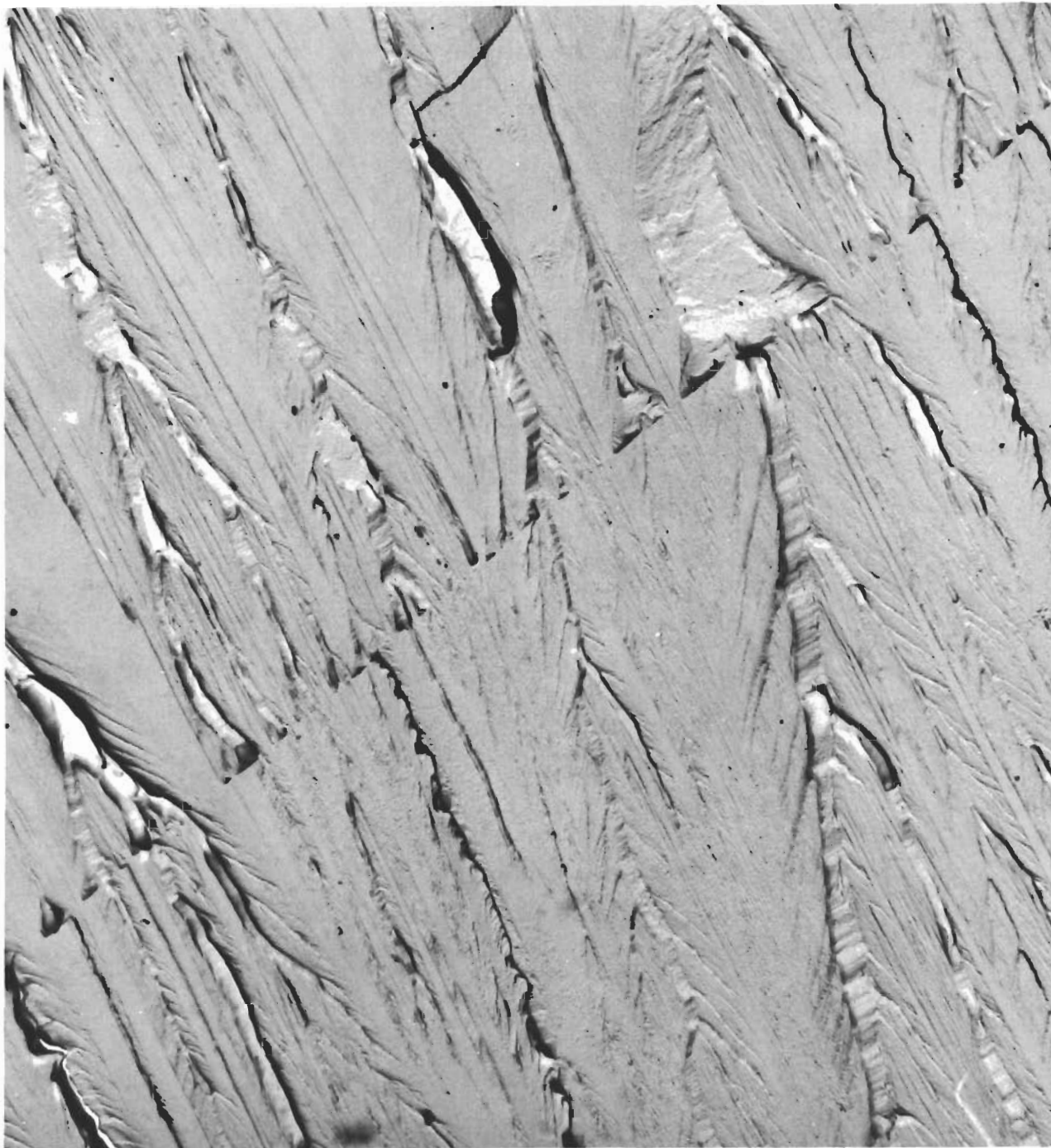


Fig. 15 Electronmicrograph of (211) cleavage in AgMg of near stoichiometric composition. 8400X

other fractographs obtained are common to those found in other brittle materials.<sup>(24)</sup> The general course of the fracture of Fig. 15 is from lower right to upper left. A low-angle subgrain boundary traverses the field from lower left to upper right. The most striking feature of the fractograph is a typical "river pattern" of fine cleavage steps. Many new steps were initiated when the fracture crossed the subgrain boundary. Large offsets between generally parallel cleavage surfaces exhibit two aspects. That on the right of Fig. 15 above the subgrain boundary shows no crystallographic features and may be ductile tearing. That on the right immediately below the subgrain boundary (as well as elsewhere less prominently) shows many fine markings at approximately 90 degrees to main markings parallel to the fracture direction. These fine markings are apparently secondary cleavage. A final item to be noted are some narrow ribbons, featureless but with straight parallel sides. Examples of such ribbons are to be found in the extreme lower-left corner of Fig. 15 and just to the right of the large offset at the lower right. These may be instances of twinning associated with the cleavage process. No evidence of twinning was ever found, however, in metallographic studies of polished sections.

## B. The Intermediate Temperature Region

From about 150° to about 350°C, although the deformation mechanism is still slip, the tensile behavior of AgMg is dominated by what appears to be a DISA phenomenon. All of the usual characteristic observations are found:<sup>(21, 25)</sup> deviations from monotonic stress-temperature curves, maxima in strain rate sensitivity-temperature curves, minima in strain hardening coefficient-temperature curves, a strong yield point, inverse yield points in rate change tests, serrated stress-strain curves (the Portevin-LeChatelier effect), strain aging behavior, and strong stress relaxation effects. This evidence is presented in the next series of figures.

### 1. Manifestations of Dislocation Interaction with Solute Atoms (DISA)

Figure 16, which reproduces typical load-elongation curves, illustrates some of the observations cited and demonstrates as well that the phenomenon is not restricted to one side of stoichiometry. The coincidence on the temperature scale of the deviation from semi-logarithmic stress-temperature behavior with the maximum in rate sensitivity and minimum in strain hardening capacity is

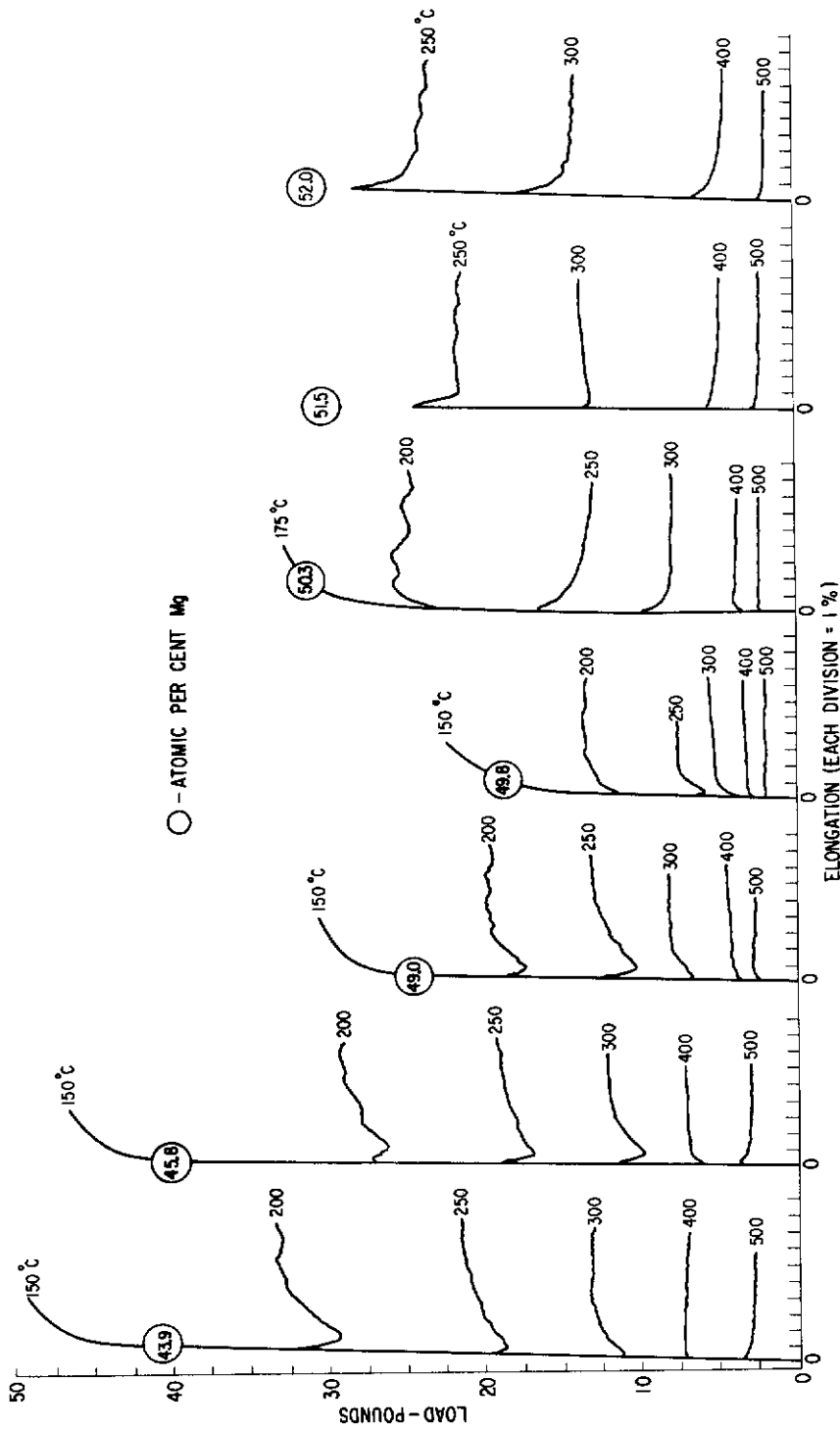


Fig. 16 Typical load-elongation curves obtained at several temperatures with a strain rate of 0.5 per cent min<sup>-1</sup> for various AgMg compounds using as specimens 0.040-inch-diameter wires with a 1-inch gage length.

shown for one composition in Fig. 17.\* Generally similar curves were obtained for other compositions. Re-examination of hardness-temperature curves previously published<sup>(9)</sup> shows positive deviation from semilogarithmic behavior similar to that seen here in the flow stress curve.

Figure 18 illustrates the phenomenon of the inverse yield point. The specimen is initially yielded at some strain rate which it will sustain without failure in the elastic region. Once yielded it can then be strained at a higher rate under which condition a new and higher yield point is established. Upon returning to a lower strain rate, however, a small dip or inverse yield point is observed before the flow curve resumes a steady course. The figure also illustrates a method for obtaining rate sensitivity at different strains on one specimen, even over a range which would not be accessible on a virgin specimen. Strain aging effects are also readily demonstrated with tensile flow curves. A specimen loaded through the yield point and immediately reloaded as in Fig. 19(a) and (b) will not show a second yield point. If, however, it is subjected to an appropriate aging heat treatment prior to reloading, a yield point will again appear as shown in Fig. 19(c).

Materials exhibiting DISA phenomena customarily show strong relaxation effects. Qualitative observation of such effects in AgMg was made in the following manner: A specimen was loaded under certain conditions of temperature and strain rate, and the stress for the upper yield point noted. Similar specimens were then loaded to various fractions of the upper yield stress, the head motion of the test machine stopped and the stress relaxation followed on the autographic recorder. A series of relaxation curves has been superposed to form Fig. 20. A marked delay time for initiation of plastic flow is implied by these results, but no experiments explicitly aimed at this effect were performed. Delay times have been observed in other intermetallic compounds, however.<sup>(26-29)</sup>

Some pre-yield micro-strain evidently occurs in the intermediate temperature range according to two types of observations. Specimens which ultimately show a pronounced yield drop at high stresses, exhibit, in an earlier

\*Rather than go through the laborious procedure of deriving the coefficients  $m$  and  $n$  from reduced true stress--true strain data, assessment of the strain hardening capacity and strain rate sensitivity for this figure were made using the roughly comparable parameters  $M$  and  $N$  where

$$M = \frac{\sigma_{\epsilon = 0.08} - \sigma_{\epsilon = 0.002}}{\sigma_{\epsilon = 0.002}}, \quad \dot{\epsilon} = K$$

$$N = \frac{\sigma_{10\dot{\epsilon}_1} - \sigma_{\dot{\epsilon}_1}}{\sigma_{\dot{\epsilon}_1}^2}, \quad \epsilon = 0.002 \text{ where } \dot{\epsilon}_1 = 0.5\% \text{ min}^{-1}$$



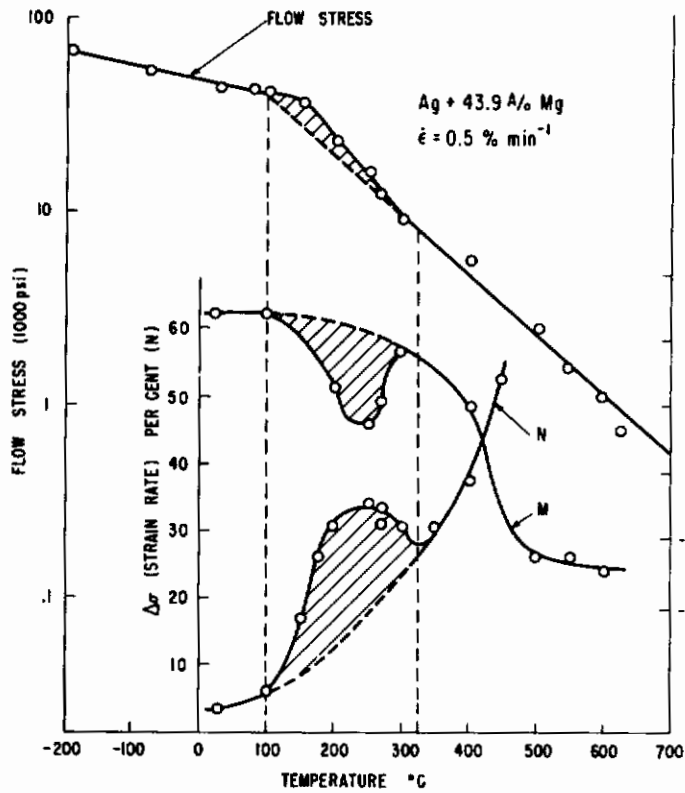
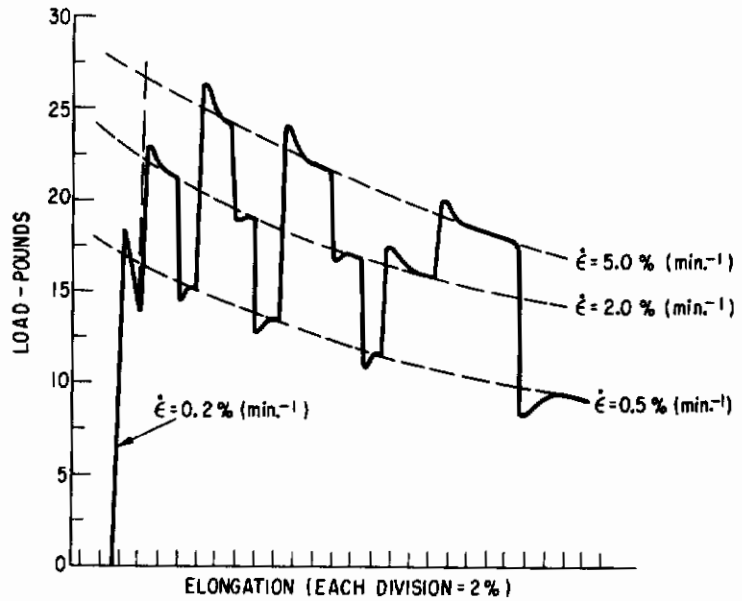


Fig. 17 Flow stress, increase in flow stress resulting from a 10X increase in strain rate, and increase in flow stress after 8 per cent elongation-- shown for 43.9 A/o Mg as a function of temperature with a base strain rate of 0.5 per cent min<sup>-1</sup>.

Fig. 18 Load-elongation curve obtained at 250°C for 51.2 A/o Mg with a specimen of 0.040-inch-diameter and 1-inch gage length, showing yield points and "inverse yielding" associated with changes in strain rate.



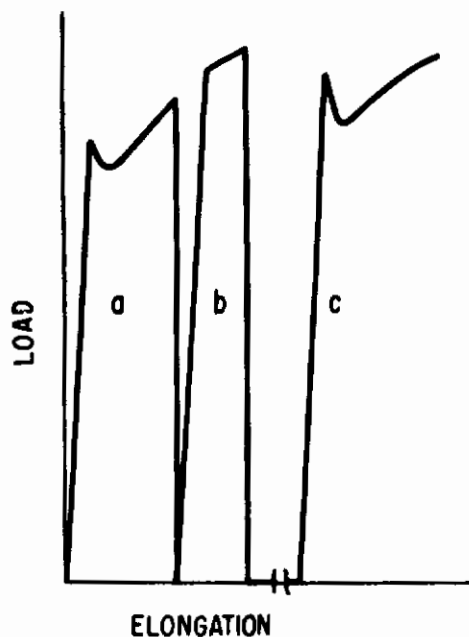


Fig. 19 Typical load-elongation curves showing strain aging phenomenon: (a) initial loading; (b) immediate reloading; (c) re-loading after aging.

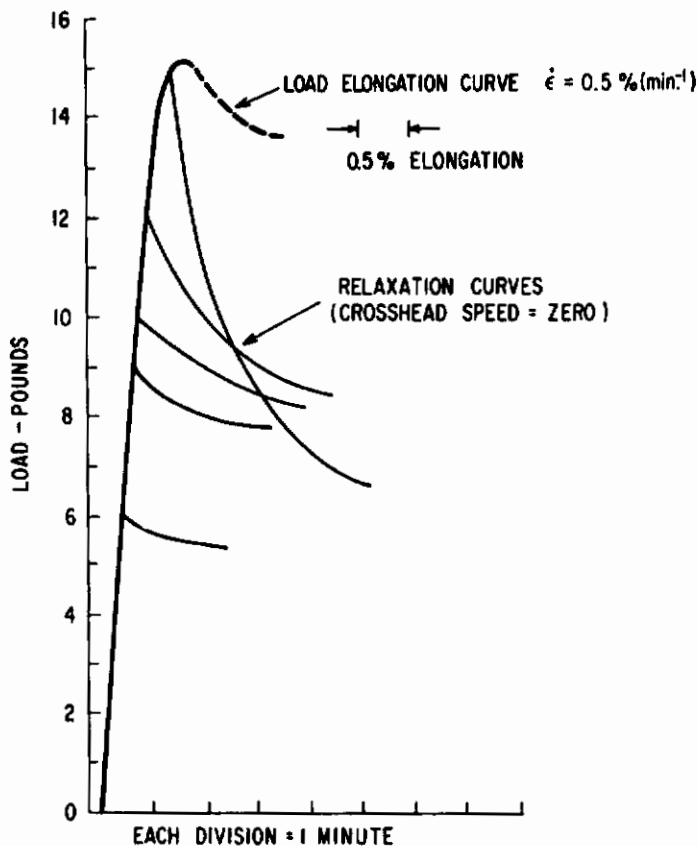


Fig. 20 Load-time relaxation curves (together with a load elongation curve) for 51.2 A/o Mg at a temperature of 270°C.

part of the stress-strain curve, momentary arrests of the recording pen. Secondly, while at low temperatures stress-strain behavior is essentially Hookean, in the intermediate temperature region the pre-yield portion of the stress-strain curve becomes much more curvilinear; i. e., the proportional limit is a much smaller fraction of the yield stress.

2. Analyses of Temperature and Rate Effects

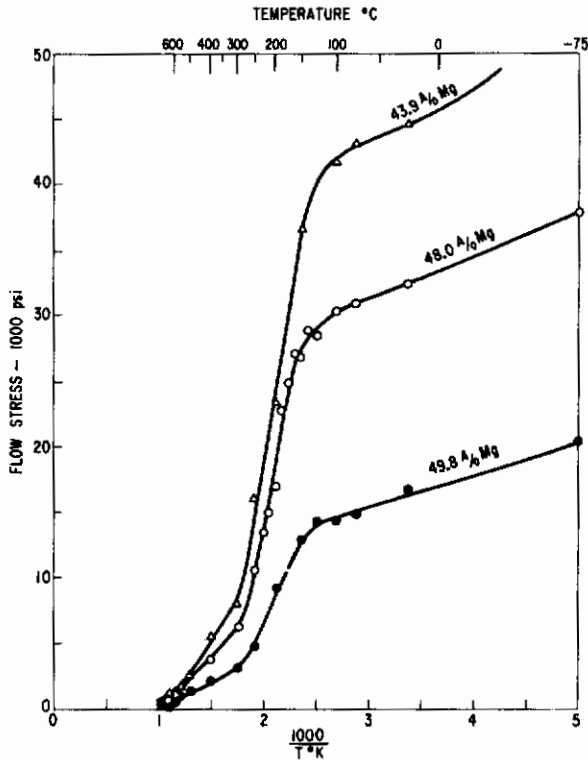


Fig. 21 Flow stress as a function of the reciprocal of the absolute temperature for various AgMg compositions.

Some theories of DISA phenomena include a reciprocal temperature dependence of yielding.<sup>(30,31)</sup> An attempt was made to test this feature of the theories using data from the present investigation; the result is shown in Fig. 21. The data are too few to provide an adequate test of the point in question, but there is a tendency toward linearity in the temperature range expected and the pattern of the curves does sharply separate the 150° to 350°C range from those temperature ranges above and below.

Since the fundamental step in any DISA process is an atomic segregation and, therefore, presumably an activated process, it is expected that equivalence of the effects of strain rate and temperature on flow stress may be demonstrated through the use of the relation

$$\dot{\epsilon} = \dot{\epsilon}_0 e^{-E/RT} \quad (3)$$

where  $\dot{\epsilon}$  is the strain rate at a temperature T,  $\dot{\epsilon}_0$  is the reference strain rate, E is the activation energy, and R the gas constant. An exponential

dependence of stress on strain rate is assumed, and flow stress-strain rate data at constant temperature are plotted as logarithm stress vs logarithm strain rate, as is shown for a typical example in Fig. 22. The near parallelism of such curves over the temperature range 225° to 300°C indicates that the activation energy in this temperature range is not greatly stress dependent. Calculation of the activation energy is accomplished by arbitrarily selecting a base temperature, assuming an activation energy, and adjusting the strain rates for the other temperatures by the use of Eq. (3). Such temperature compensated strain rate-flow stress data are plotted together with the base temperature curve, and a best fit value for the activation energy obtained by successive re-approximations of the value used in

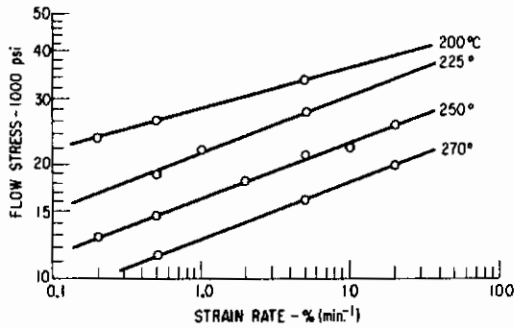


Fig. 22 Variation of flow stress with strain rate at various temperatures for 51.2 A/o Mg.

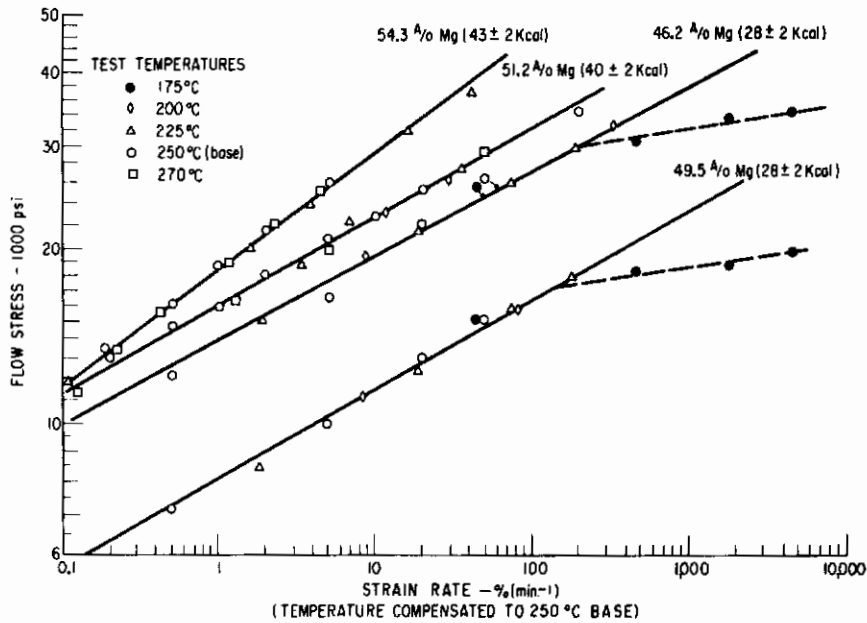


Fig. 23 Curves of flow stress vs strain rate (temperature compensated to a 250°C base) showing the best fit of points in the determination of energies involved in the flow process.

relation (3) to adjust the strain rates. Application of this technique to four AgMg compositions over the temperature range in question is shown in Fig. 23. The conformance with the hypothesized relations is considered quite satisfactory. Deviation of points at the highest (temperature compensated) strain rates and the low end of the temperature range is to be expected.

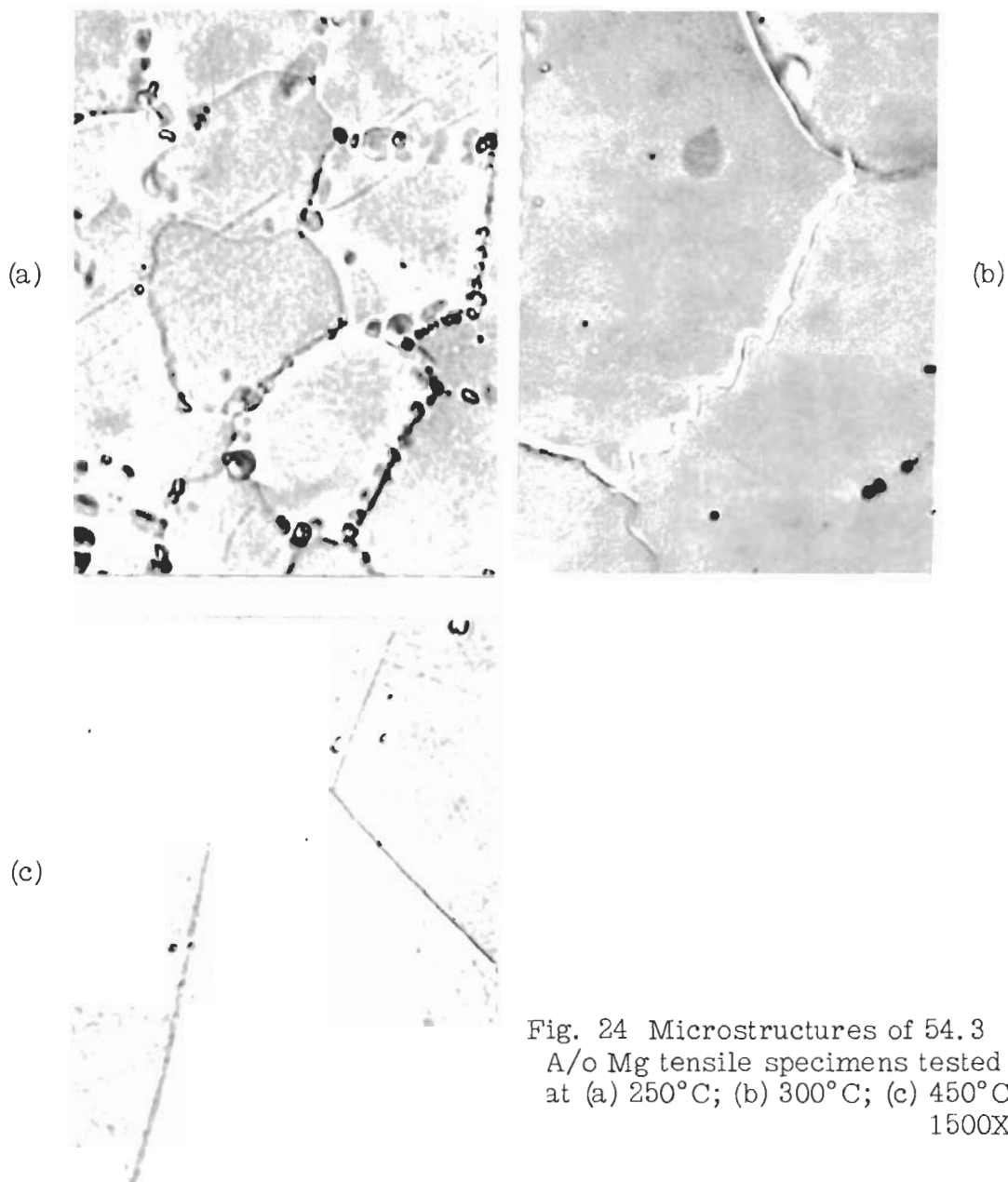


Fig. 24 Microstructures of 54.3 A/o Mg tensile specimens tested at (a) 250°C; (b) 300°C; (c) 450°C. 1500X

There are two additional points of interest in Fig. 23. First the slope of the  $\log \sigma - \log \dot{\epsilon}$  curve for the 54.3 A/o Mg alloy is markedly greater than the others. This composition had been judged single phase upon initial metallographic examination, but careful re-examination after testing in the 150° to 450°C range, revealed evidence of grain boundary precipitation of a second phase for tests in the lower part of this temperature range, as is shown in Fig. 24(a). Much solution

takes place during the time of test at 300°C, but the pronounced jagged appearance of many boundaries, Fig. 24(b), indicates that the motion of the boundaries is still impeded by particles. It was found that the impeding particles could be dissolved above 400°C, approximately the solvus for the 54.3 A/o composition, leaving clean grain boundaries as is shown in Fig. 24(c). The instability of the two-phase material, by solution and/or agglomeration of the second phase, reveals itself in both a fictitiously high activation energy and in an anomalous stress-strain rate relationship. Data for the 54.3 A/o Mg alloy in this temperature range, therefore, are not considered further.

The other point to be noted in Fig. 23 is the marked effect of defect structure on the energetics of the pinning process. Excess silver atoms give values of the order of 28 kcal while excess magnesium atoms give about 40 kcal. Energies of the order of 28 kcal were also found for 43.9 and 49.0 A/o Mg, and values of the order of 40 kcal for 50.3 and 51.5 A/o Mg.

### 3. Grain Size Effects

Grain size effects have also been observed in this temperature range. Some of these results are shown in Fig. 25. It is believed that these effects are primarily a reflection of the interaction between grain size and the DISA phenomena since the size dependence is the inverse of that for normal slip and decreases with increasing temperature in this range.

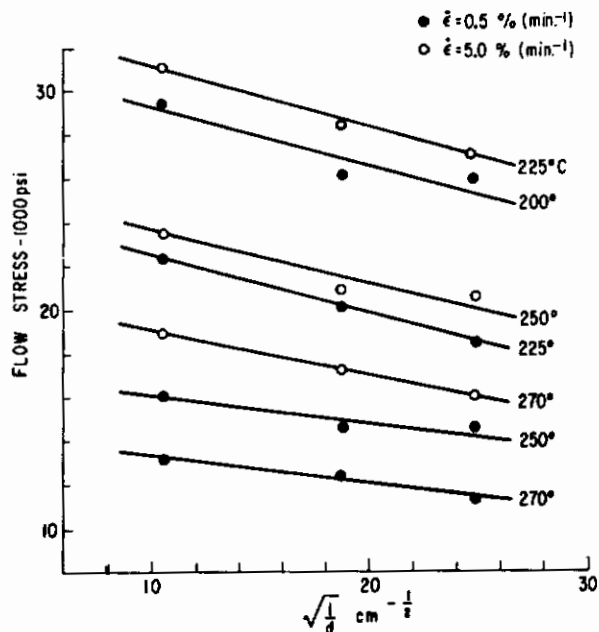


Fig. 25 Flow stress of 51.2 A/o Mg as a function of the square root of the reciprocal of the grain diameter for various test temperatures.

C. The High-Temperature Region

1. Observations on Flow Stress

(a) Effects of Temperature and Composition. The temperature range above about 400°C is characterized principally by a high dependence of the flow stress on both temperature and strain rate. Such a dependence is probably indicative of diffusion controlled deformation. Figure 26, an extension of the flow stress-composition isotherms of Fig. 3, not only illustrates the effect of temperature but also demonstrates a changed role of lattice defects. It is to be noted also that data for the 54.3 A/o Mg alloy are plotted for temperatures of 500°C and higher since the alloy at these temperatures could be assumed to be in the solid solution condition. The general effects of temperature on the 0.2 per cent offset flow stress over the whole range of temperature for some representative compositions are shown in Fig. 27. It will be observed that because of the incidence of DISA effects the data fail to conform to the semilogarithmic behavior often noted for stable materials.

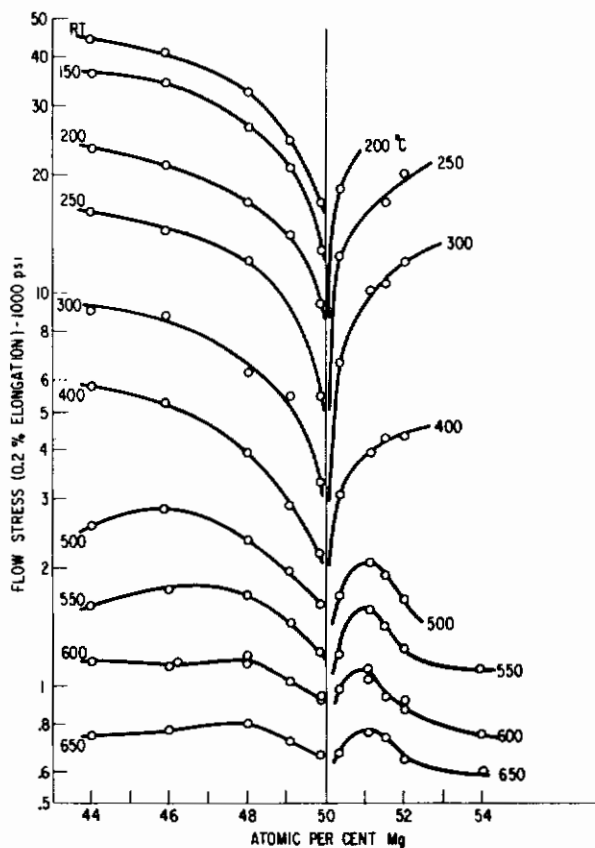


Fig. 26 Flow stress isotherms as a function of composition for AgMg (extended to higher temperatures from Fig. 3).  $\dot{\epsilon} = 0.5$  per cent  $\text{min}^{-1}$ .

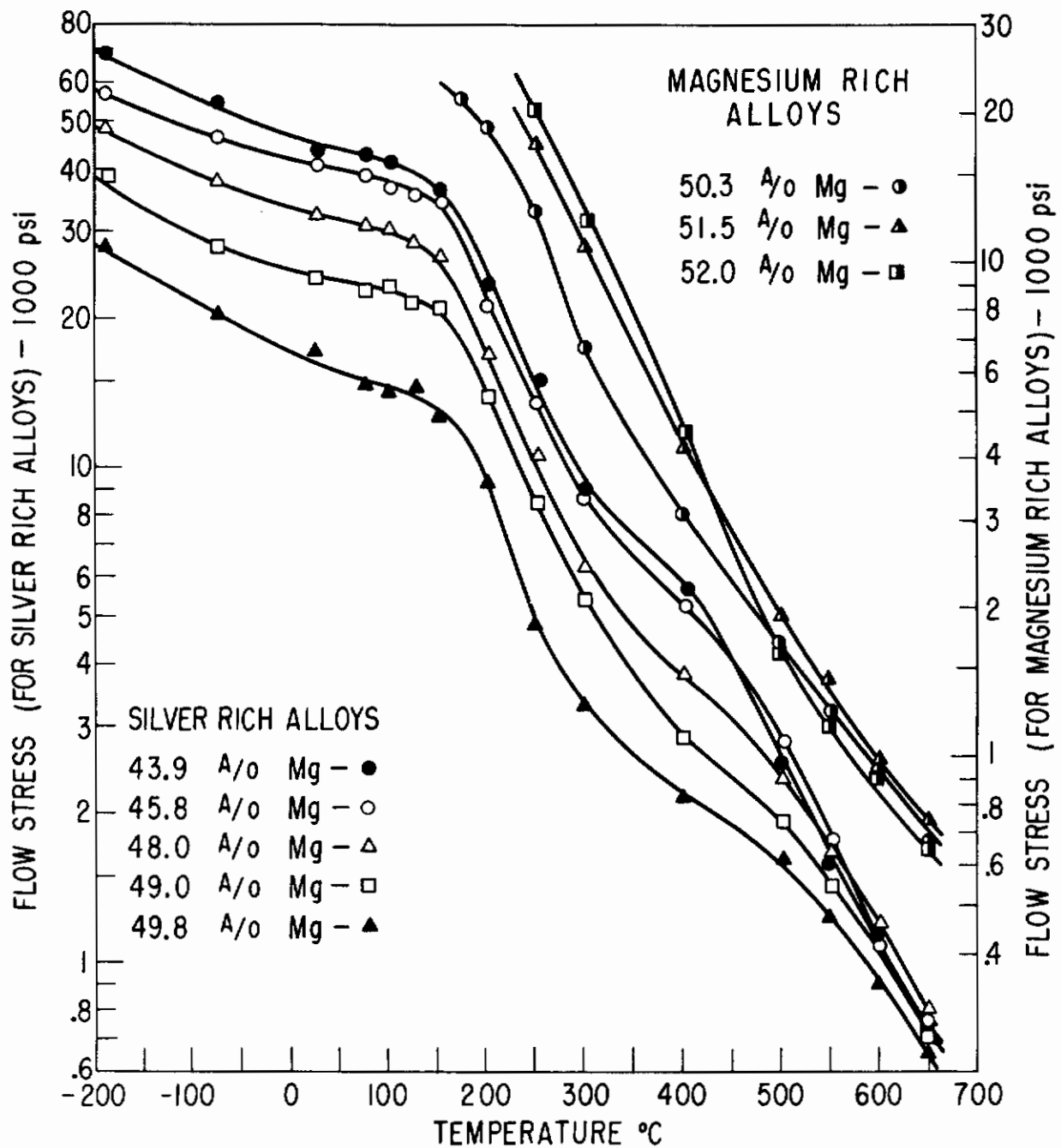


Fig. 27 Flow stress of both Ag-rich and Mg-rich compounds as a function of temperature.  $\dot{\epsilon} = 0.5$  per cent  $\text{min}^{-1}$ .



(b) Effects of Strain Rate. A representative example of the effect of strain rate on the flow stress is shown for various temperatures in Fig. 28. Again, assuming deformation in this range to be an activated process, an attempt was made to reduce the data to a single line plot with a temperature compensated strain rate parameter in a manner analogous to the treatment of similar data in the intermediate temperature range. Good results were obtained as is shown in Fig. 29; only for the lowest temperatures and highest strain rates do the data points deviate from a single straight-line representation.

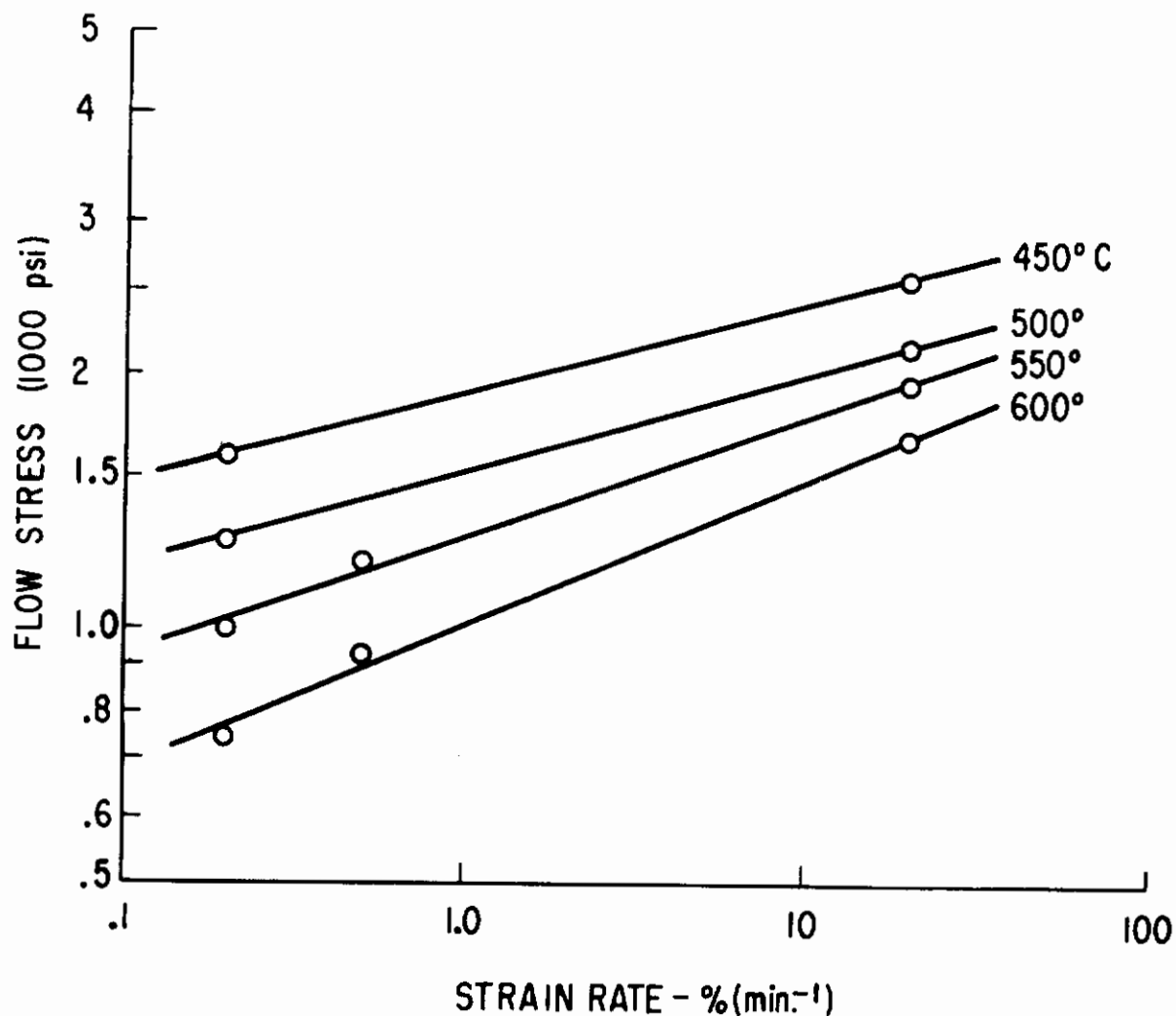


Fig. 28 Effect of strain rate on the flow stress of 49.8 A/o Mg at several temperatures.

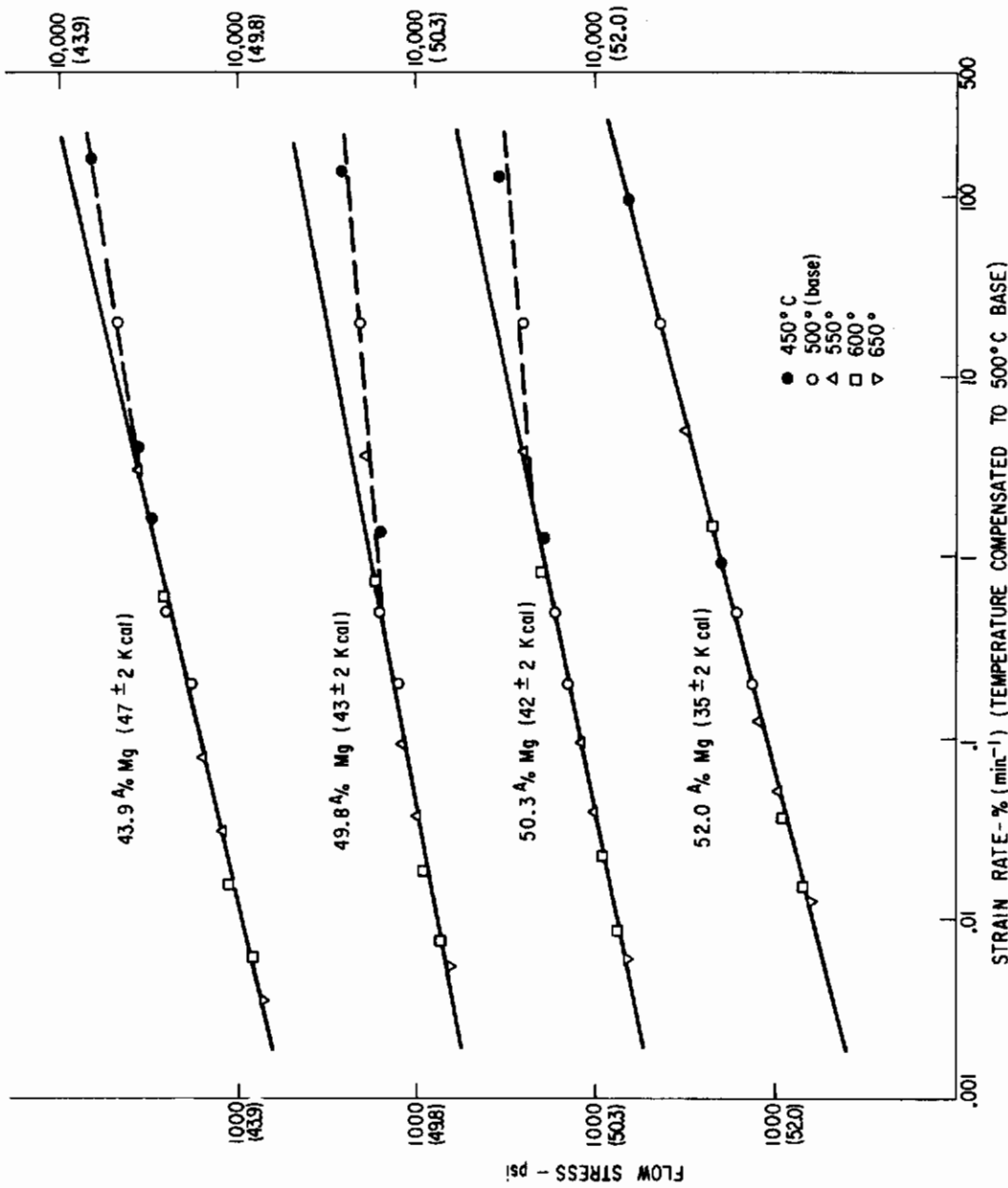


Fig. 29 Curves of flow stress vs strain rate (temperature compensated to a 500°C base) showing the best fit of points in the determination of energies involved in the flow process.

(c) Effects of Grain Size. The effects of grain size at the lower end of the high-temperature range are negligible as is to be expected since this is the normal equi-cohesive range on the homologous scale. Grain size effects could not be examined at the highest test temperatures employed, since only coarse-grained structures (annealed at 600°C) remained stable at the test temperature.

(d) Effects of Strain. In a study of the effects of strain on the flow stress it was found that in the high temperature region the stress at  $\epsilon = 0.08$  as a function of composition was strikingly similar in appearance to Fig. 26. Calculations of the strain hardening exponent  $m$  showed that the values for  $m$  are positive but quite close to zero.

## 2. Other Observations

Further observations consistent with the above behaviors may be cited. The previous recrystallization study of a cold-worked single crystal of near stoichiometric composition showed that appreciable recovery occurred during a 1-hour anneal at temperatures as low as 150°C. Recrystallization was essentially complete after annealing for 1 hour at 250°C ( $\sim 0.5 T_{mp}$ ). It is not surprising, therefore, that microstructures of material extruded at  $\sim 500^\circ\text{C}$  or tested in tension at temperatures of 400°C or higher are typical hot-worked microstructures with little or no evidence of a deformation texture.

Both silver-rich and magnesium-rich wires were found to be very ductile in the high-temperature range. Elongations of 100 per cent or more were common; scatter in the total elongation data, however, precluded any quantitative treatment of the results. Fractures of both Ag-rich and Mg-rich specimens were predominantly intercrystalline.

## IV. DISCUSSION OF AgMg RESULTS

The results of this investigation have been presented in terms of the models and mechanisms which are believed to best represent the observed behaviors. It would be well, however, to mention some of the other models which have been proposed as strengthening mechanisms in intermetallics and to cite reasons for the lack of pertinence of these models to the present study.

### A. The Low-Temperature Region

#### 1. Considerations of Flow Stress

(a) Effects of Composition. Various metric, morphic, and steric effects of the state of long-range order on the mechanical properties of intermetallics have been predicted and observed in a variety of previous studies [for a review see (1)].

Although the state of long-range order is both very high and essentially independent of temperature in this region,<sup>(32, 33)</sup> it is dependent on composition. This composition dependence is complex in that both metric and steric factors are involved. Even in the absence of any metric differences between silver and magnesium atoms, the chemical differences in the two species can still give rise to steric effects of changes in long-range order as the composition departs from the equiatomic ratio. To a first approximation, however, the degree of long-range order is expected to be a linear function of composition. Thus, if the elastic analysis of Shibuya<sup>(34)</sup> applies,\* the flow stress at a constant temperature would be expected to be linear with the deviation from stoichiometry,  $\Delta$ . On the other hand, Brown's model of a diffuse antiphase domain boundary<sup>(36)</sup> would require at constant temperature a square law dependence on  $\Delta$  with the same approximation. Since the experiments clearly demonstrate that  $\sigma$  is proportional to  $\Delta^{0.27}$ , it is apparent that still other considerations must be taken into account for the behavior of AgMg.

One obvious factor, already introduced in the presentation of the results, is the metric difference between the silver and magnesium atoms. Stoichiometric AgMg was likened to a metallic solid solution with excess silver and magnesium atoms as substitutional solutes. This approach was successful in accounting for the general order of strengthening effects due to substitution of Ag and Mg as well as ternary elements. Size effects alone, however, cannot account for the fractional power dependence on  $\Delta$ , since a normal metallic solid solution is hardened approximately as a linear function of solute concentration, i. e., lattice distortion.<sup>(10)</sup> A simple additive combination of the steric and metric factors would still be linear with solute concentration. Clearly, then, to account for the results, refinements in the theoretical treatments must be made, perhaps to include interaction effects between steric and metric factors.

One complication is suggested by the following observation: The previous study of the indentation hardness<sup>(9)</sup> of AgMg showed its composition dependence at low temperatures to be approximately linear whereas both the initial (lower yield) flow stress and the flow stress at moderate strains ( $\sim 8$  per cent) exhibited a fractional power dependence. Such a comparison is shown in Fig. 30 in which the hardness data shown were taken on wires of the same batch from which the tensile specimens were obtained. According to Tabor<sup>(38)</sup> a strain of 0.08 should be a valid point of comparison for Vickers hardness and tensile data. It is suggested that the difference in the two types of measurements may involve effects of grain boundaries since the hardness results were, in effect, obtained on single crystals (low load measurements such that each indentation fell within the compass

---

\*A linear dependence of strength on long-range order is realized in Ardley's experiments on stoichiometric  $\text{Cu}_3\text{Au}$  where change in long-range order could be attained without change in composition.<sup>(35)</sup>

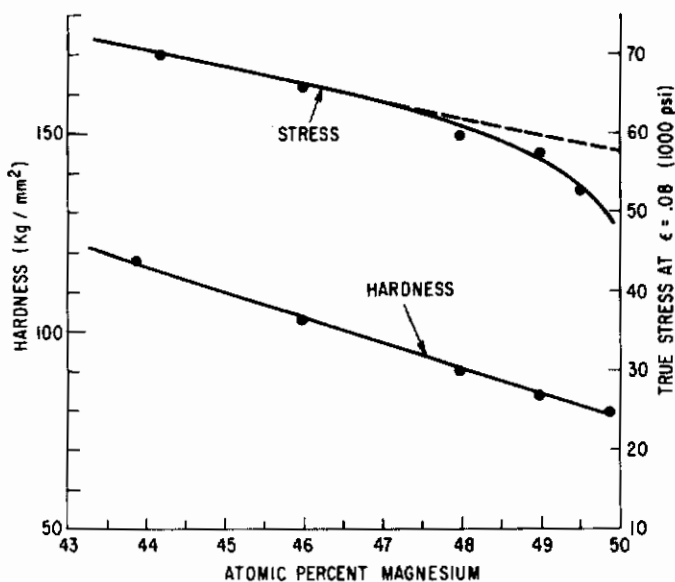


Fig. 30 Hardness and stress (at  $\epsilon = 0.08$ ) at RT as a function of composition for material of grain size  $\sim 1.7 \times 10^{-3}$  cm. (Each hardness value is the average of 10 indentations, each made in a different randomly selected grain.)

of a single grain) whereas the tensile flow stresses were obtained on polycrystalline specimens. Some support for this notion is afforded by a pair of studies on the solution hardening of magnesium metal. Levine, Sheely, and Nash<sup>(39)</sup> made measurements on single crystals and found a linear dependence of flow stress on composition. Hardie and Parkins,<sup>(40)</sup> on the other hand, in their work found a definite curvilinear behavior. A reassessment of their results shows fair conformance with the empirical formula  $\sigma = K\Delta^s$  used here to describe solute effects in AgMg; a value for  $s$  of the order of 0.2 was again obtained. Analogous single-crystal studies in AgMg are clearly desirable to pursue this possibility.

(b) Effects of Domains. In many intermetallics, antiphase domain structures play a role with maximum strength occurring at an optimum domain size according to analyses by Cottrell<sup>(41)</sup> and Logie.<sup>(42)</sup> Since the CsCl structure of AgMg has only two types of atomic sites, any domain structure resulting from initial ordering will be highly unstable and will disappear almost immediately by thermal activation at all ordinary temperatures.<sup>(43,44)</sup> While no explicit attempts were made either to measure or alter any existing domain structures in the present investigation, it is not believed possible to account for any of the observations in this way.

(c) Effects of Grain Size. The inability to obtain consistent effects of grain size in the low-temperature region cannot be ascribed to experimental errors in testing or to uncertainties in grain size determination. Rather, it is believed

that the grain sizing heat treatments have complicated the situation by the formation of solute atmospheres about certain dislocation sites as well as by affecting the nature of the dislocation substructure.<sup>(45)</sup>

There is, in fact, some evidence which might be taken as indicative of possible complexing by an atmosphere effect. The samples of the finest grain size ( $\sim 1.7 \times 10^{-3}$  cm) were as-extruded samples. Such samples, as a result of normal processing, had been cooled rather quickly from the extrusion temperature ( $\sim 500^\circ\text{C}$ ) and were consistently weaker at low temperatures than samples of the next coarser grain size ( $2.8 \times 10^{-3}$  cm) prepared by heat treating as-extruded material at  $400^\circ\text{C}$ . Perhaps, then, all samples but those of the finest grain size (tested in the as-extruded condition) are strengthened by the presence of atmospheres formed during the grain growth anneals. The fact that annealing of as-extruded samples, prior to testing, at  $250^\circ\text{C}$  (a temperature too low to cause significant grain growth), resulted in somewhat increased flow stresses is indicative of the formation of dislocation atmospheres. The inability of such an annealing treatment to give sufficiently increased flow stress to satisfy the theoretical dependence of flow stress on grain size suggests that at  $250^\circ\text{C}$  the atmosphere formation is slow and was only partially accomplished.

(d) Effects of Strain. Another unanswered problem lies in the work hardening characteristics. It is often contended that one reason that intermetallics are brittle is that they work harden rapidly. Two specific models have been suggested. That of Flinn<sup>(46)</sup> depends on the existence of a stable domain structure and is not pertinent for the reasons discussed above. Brown,<sup>(47)</sup> on the other hand, extends the theory of Shoenck and Seeger<sup>(48)</sup> and suggests that, in any ordered compound, the usual ability of a cross-slip process to decrease the work hardening tendency is impaired by the extended character of the super dislocation. This contention, however, is not borne out by the present experiments. Stoichiometric AgMg was found to work harden no more rapidly than many pure metals at the equivalent homologous temperatures. It was observed, in fact, that off-stoichiometric compositions work hardened even less rapidly than is typical for many metals.

## 2. Considerations of Ductility

(a) Effects of Prestrain. One of the most intriguing observations arising from the present study (and perhaps that of greatest practical significance) was that an extruded silver-rich wire is ductile at room temperature while the same composition in the as-cast condition is completely brittle. Explanations based on grain size can be ruled out because grain sizes equivalent to those in cast material can be produced by post-extrusion anneals without embrittling the sample. Deleterious effects of compositional heterogeneities can also be ruled out because homogenization heat treatments do not enductile cast samples. Presence of a

favorable crystallographic texture in as-extruded material is plausible, as discussed above, but the high extrusion temperature would tend to minimize its formation. Actually, very little texture was found in x-ray analyses. It might be argued that deformation enductiles by virtue of mechanically disordering the material, thereby removing whatever impediment that long-range order presents to the flow process. Some superlattice reflections, however, can be seen in x-ray diffraction photographs of ductile as-extruded wires. Furthermore, wires given post-extrusion low temperature heat treatments remained ductile while showing excellent x-ray pictures with all superlattice lines strong and sharp.

Perhaps, then, the improved properties of extruded material may be attributed to beneficial effects of prestrain per se. In this light, the observations on AgMg are strikingly reminiscent of the so-called "rheotropic" behaviors observed in steels<sup>(49-53)</sup> and zinc,<sup>(54)</sup> and utilized in the commercial production of tungsten and molybdenum<sup>(55,56)</sup> wire. In all of these cases, deformation of a non-face-centered cubic metal under ductile conditions has been demonstrated to improve its ductility at low temperatures, high strain rates, or under superposed hydrostatic tensile stresses. That portion of the brittleness occurring under severe testing conditions which is strain curable has been designated "rheotropic" brittleness. Figure 31 adapted from one due to Ripling<sup>(52)</sup> illustrates schematically the rheotropic phenomenology. Curve A is a typical transition temperature curve as a function of one of the embrittling variables. The lower level ductility is raised from  $\epsilon_A$  to  $\epsilon_B$  by the action of the prestrain  $\epsilon_S$  or, alternatively, the transition temperature of the prestrained material, as shown for example by curve C, is lowered a corresponding amount,  $\Delta T_T$ . The rheotropic embrittlement area is shown by the diagonal shading in Fig. 31.

If reference is made to Fig. 13, it will be seen that the results of the present study can be similarly regarded. The initial extrusion processing has lowered the transition temperature for Ag-rich compositions to the order of  $-100^\circ\text{C}$  and for Mg-rich specimens to about  $200^\circ\text{C}$ . High-temperature tensile deformation of Mg-rich specimens evidently lowered their transition temperature to a value well below room temperature. The beneficial effects of a low strain rate for initial yielding on subsequent deformability at higher rates (see Fig. 18 and associated text) can also be viewed as a lowering of the transition temperature.

No detailed mechanistic model for rheotropic recovery is yet at hand. Ripling et al. have demonstrated that rheotropic behaviors are obtained with both tensile and compression prestrain<sup>(51)</sup> and are influenced by, but not caused by, conventional strain aging.<sup>(52)</sup> Presumably, then, the true model involves some solute-dislocation structure interaction. Perhaps high-temperature deformation followed by a rapid cool, as in the extrusion process, leaves a residue of dislocations which remain mobile at room temperature because atmospheres have not formed. Such reasoning would require, however, an explanation for the lack of embrittlement of extruded wires during grain size annealing.

In an analogous manner, however, Ripling<sup>(52)</sup> found that rheotropic recovery of a high-strength steel persisted through a second tempering (or aging) treatment up to at least the initial tempering temperature.

Still other consistencies may exist between metals showing a ductile-brittle transition temperature and the compound AgMg. Magnusson and Baldwin<sup>(57)</sup> have analyzed the behavior of a large number of non-face-centered cubic metals which become brittle at low temperatures and high strain rates. A schematic diagram due to these authors is reproduced in Fig. 32. For a number of these metals

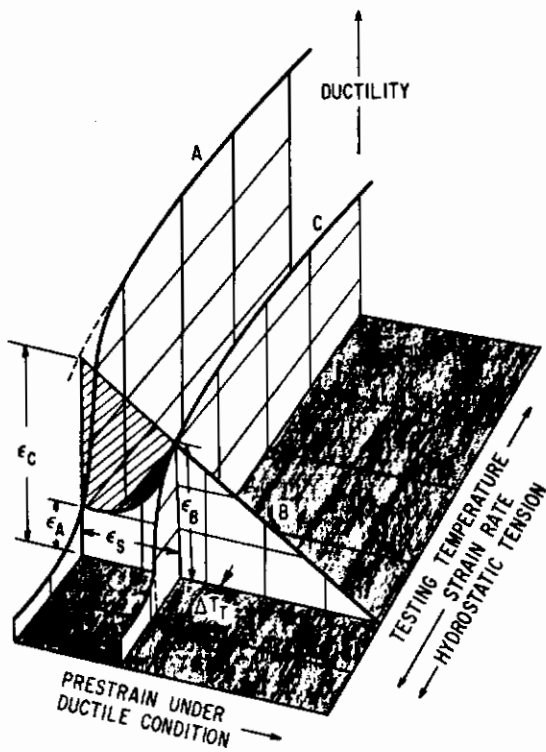


Fig. 31 Schematic representation of the rheotropic embrittlement phenomenon showing the effects of prestrain, temperature, strain rate and stress state on ductility [after Ripling<sup>(52)</sup>].

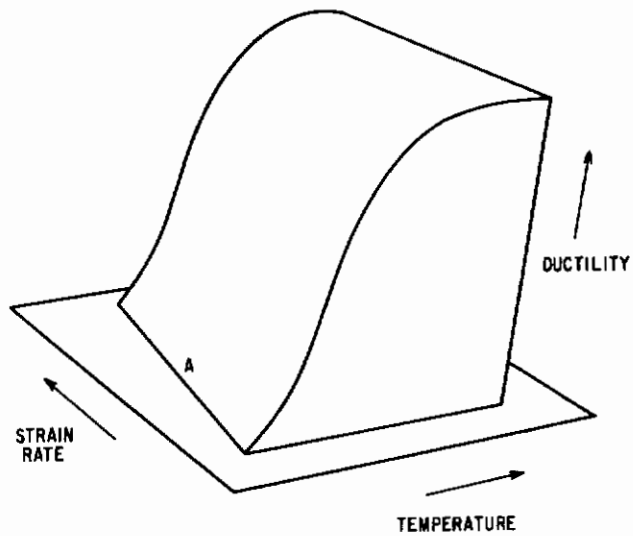


Fig. 32 Interrelated effects of temperature and strain rate on the ductility of a brittle material [after Magnusson and Baldwin<sup>(57)</sup>].



(W, Mo, Cr, Fe, Cd, and Sn) the boundary of the brittle zone (line A of Fig. 32) has been found to be linear if strain rates are plotted logarithmically against reciprocal absolute temperature; i. e.,  $\dot{\epsilon} = Ae^{-U/KT}$ . A is a constant  $\approx 10^{12} \text{min}^{-1}$  which is essentially independent of the identity of the metal,\* grain size, or test condition. The ductility data at hand for AgMg are too crude to permit evaluation of this feature but the general trend seems to be followed.

(b) Effects of Composition. The observations of the effects of composition on room temperature ductility of extruded wires inspire speculation as to their origin. Both electronic and metric factors may be considered. The former are of doubtful pertinence according to the following rationale. Let it be assumed that deformation at ordinary temperatures is possible only if the electron/atom ratio is below some value, say, 1.5. The brittleness of magnesium-rich samples and those containing tin is then accounted for because each excess magnesium atom contributed two electrons per atom and tin, four (if tin be reckoned as electropositive) and the electron/atom ratio of the stoichiometric base is already 1.5. However, zinc also contributed two electrons per atom and the zinc addition failed to embrittle the compounds.

Possible metric factors may now be considered. It will be recalled that both excess magnesium and ternary additions of tin caused the lattice to expand and that both types of addition embrittled AgMg at room temperature. On the other hand, silver and zinc (contracting additives) could be alloyed without marked effects on ductility. Perhaps this particular lattice will withstand some contraction but is intolerant of any substantial expansion. Such an explanation is still doubtful, however, since the Ag/Mg ratio in the ternary alloys was so close to unity. Experiments are needed in which sufficiently large amounts of Sn are added to a definitely Ag-rich base to cause a net expansion or sufficiently large amounts of Zn to a definitely Mg-rich base to cause a net contraction. According to the hypothesis now being considered the former should embrittle while the latter might enductile the binary alloy.

Another line of reasoning concerning the effect of composition on ductility may also be introduced. While the flow stress may be conditioned primarily by the mean effective lattice strain distributed over the whole lattice, it is possible that fracture is determined by the local strain about substituted excess atoms. If such be the case, then a relatively small amount of highly distorting atoms would embrittle while additions of weakly distorting atoms, corresponding to much larger changes in mean lattice parameter, would fail to do so. Unfortunately, the available data fail to permit distinction between sign or numerical magnitude of the local distortion as the important factor. Tin and magnesium are not only

---

\*Zinc is an anomalous exception with a value for  $A \approx 10^{32} \text{min}^{-1}$ .

large atoms but they also impart larger lattice strain per atom per cent addition than do the two small atoms studied, silver and zinc. Experiments with small additions of highly contracting solutes might be used to test this hypothesis.

### 3. Considerations of Fracture Mode

Another puzzling question is the overwhelming tendency of AgMg wires to fail intergranularly at all temperatures and for all compositions. The proper explanation must lie in one of two categories: either grain boundaries are inherently weaker than bulk material, or grain boundaries by some means concentrate stress to an extraordinary degree. Two of the usual explanations, one in each category, must be ruled out. The apparent weakness of grain boundaries is frequently traceable to the presence of a brittle second phase distributed along the grain boundaries. Careful metallographic examination of boundaries of the AgMg samples at high magnification disclosed no trace of a second phase. In an explanation of the second category, grain boundaries are often thought of as constituting a barrier to dislocation passage thereby causing a pile-up of dislocations and consequent stress concentration. The barrier qualities of grain boundaries supposedly derive from the difficulties in propagating slip in the adjoining grain which will usually not be favorably oriented for slip. While this model accounts for the fact that coarse-grained samples are more brittle than fine-grained samples, the observation that all three slip planes {321} {211} {110} are usually operative (a total of 42 possible slip systems) would seem to lessen considerably this aspect of barrier formation. Another possibility which should be investigated is that of grain-boundary composition gradients.<sup>(58)</sup> Mechanisms by which such gradients could lead to intergranular failure could be propounded under either of the two general categories above. A necessary first step would be experimental proof that concentration gradients exist at boundaries. The electron beam micro-probe affords an excellent opportunity for such an investigation.

### B. The Intermediate Temperature Region

#### 1. Considerations of Flow Stress

It is believed that the evidence presented is overwhelmingly indicative that some sort of DISA phenomenon dominates the intermediate temperature range. One of the features noted, albeit not a prominent one in this instance, is the increased flow stress within the intermediate temperature range. Increases in hardness or flow stress at moderately elevated temperatures have been noted many times before in intermetallic compounds, and a variety of models have been proposed to explain such strength peaks (for a review see Refs. 1 and 47). Among these are:

- A. Those based on the oppositely directed effects of temperature on elastic modulus and
  - 1. Domain size
- or
- 2. Long-range order.

B. Those based on the effects of diffusion on the structure of dislocations producing

1. Diffuse antiphase domain boundaries between pairs of partial dislocations [Brown<sup>(36)</sup>]
2. Non-coplanar pairs of partial dislocations; two slightly different models [Flinn,<sup>(46)</sup> Barrett<sup>(43)</sup>]
3. Failure of the trailing partial dislocation of a moving pair to restore order [Herman<sup>(59)</sup>].

The models in group A can be rejected for AgMg since, both domain structure, as described above, and long-range order, as shown by the thermodynamic studies of Kachi<sup>(32)</sup> and of Trzebiatowski and Terpilowski,<sup>(33)</sup> are essentially independent of temperature. Brown's model in group B is invalid because, in the absence of a temperature dependence of long-range order, the stress required to move a dislocation should increase approximately linearly with temperature as diffusion renders the antiphase domain boundary progressively more diffuse. Herman's model predicts that the yield stress should be very strain rate sensitive and decrease with an increase in strain rate. Since the opposite effect was observed in this study, this model, too, is discarded. In both Flinn's model and that of Barrett the stress to move a pair of partial dislocations is increased when the pair of partials become displaced from a common slip plane. This increase in stress is a result of balance between antiphase domain interfacial energy and elastic energy (Flinn) or a result of chance interaction with vacancies (Barrett). Such effects perhaps occur in AgMg but, as Flinn points out, their magnitude should be very much less in CsCl structures than in the  $L_{12}$  or  $Cu_3Au$  structure since there are some wrong bonds for all orientations of domain boundary. More importantly, no mechanism is seen whereby these models can give rise to the yield drop, inverse yielding, and Portevin-LeChatelier effects observed for AgMg. Certain of the DISA models do account both for these effects and for the increased flow stress.

Cottrell and Jaswon<sup>(8)</sup> have presented a model for the interactions between moving dislocations and moving solute atoms, i. e., those interactions occurring at low dislocation velocities or high temperatures. The essence of their argument is that there is an instability in the motion of a dislocation. A moving dislocation is slowed down by solute atoms jumping into favorable sites in the vicinity of the dislocation, more jumps are then possible at the slower speed and the dislocation rapidly decelerates as the atmosphere forms about it. Under higher stresses, the dislocation moves more rapidly, the atmosphere begins to be stripped from it, thus further accelerating the dislocation until

speeds are reached at which other effects such as thermally activated climb over obstacles become controlling. Thus, under appropriate conditions of stress and temperature, dislocation behavior should oscillate between two stable ranges of velocity--"fast" and "slow."

This explanation has been held<sup>(60)</sup> to account for the flow curve serrations or Portevin-LeChatelier effect observed for other metals and hence might be extended to AgMg.\* In addition, two further predictions were made by Cottrell.<sup>(60)</sup> Because of the accelerating effects of strain produced defects on diffusion rates, the flow curve for a metal exhibiting this type of dislocation interaction will be smooth at small strains where the diffusion coefficient,  $D$ , is small, serrated at intermediate strains where  $D$  is sufficiently large to produce the effect, and smooth again at large strains where  $D$  has increased beyond the optimum value. At lower temperatures or (in this case) with compositions close to stoichiometry the serrated portion of the curve should be displaced to higher strains. These effects are found to some extent in the intermediate range as may be seen by inspection of Fig. 16.

Cottrell<sup>(41)</sup> has also predicted the temperature at which flow curve serrations should be observed using the equation

$$D = 10^{-6} \epsilon \exp (-U/RT)$$

where  $\epsilon$  is the strain and  $U$  is the activation energy to move a solute atom into an adjacent site. Based on analyses of strain aging in iron, Cottrell assumes the necessary diffusion coefficient to be of the order of magnitude  $10^{-9} \dot{\epsilon}$ . Estimating  $U$  as one-third of the Ag<sup>110</sup> diffusion activation energy<sup>(12)</sup> and taking  $\epsilon = 10^{-2}$  and  $\dot{\epsilon} = 5 \times 10^{-3} \text{ min}^{-1}$ , temperatures for the incidence of serrated flow in AgMg alloys may be estimated. In view of the crudity of the estimates the agreement is satisfying as is shown in Table II.

An accumulation of data on the upper yield point of AgMg would have provided a basis for further analyses of the DISA phenomena. While marked differences between upper and lower yield points were frequently observed (see Fig. 16), no detailed analyses of the upper flow stresses were attempted since this

---

\*Some difficulties exist with this rationale.<sup>(61)</sup> Although the model appears reasonable in terms of a single dislocation, it is difficult to imagine how many thousands of dislocations could accelerate and decelerate in concert to give rise to macroscopic jerky flow. In addition the final expression for the flow stress given by Cottrell and Jaswon contains no temperature dependent term, as would seem to be required by the present experimental evidence.

TABLE II

A Comparison of Calculated and Observed Temperatures  
for the Incidence of Serrated Flow in AgMg Alloys

Comp A/o Mg	$Q_{Ag^{110}}$ kcal/g- atom	U kcal/g- atom	$T_{calc}$		$T_{obs}$
			$^{\circ}K$	$^{\circ}C$	
45.8	41.3	13.8	497	224	} $\sim 200^{\circ}C$
49.8	40.7	13.6	490	217	
52.0	38.0	12.7	457	184	

parameter seemed so much more erratic and irreproducible than the lower yield flow stress. In the present case, a major factor responsible for these difficulties is undoubtedly the fact that the wire samples were seldom perfectly straight so that true axial alignment in the testing machine did not occur until after yielding had taken place. It is possible to eliminate this problem, at least in part, by the following procedure: the specimen is mounted in the testing machine, the grips seated, and the specimen straightened by pulling to a very small strain. The specimen is then annealed in place and a stress-strain curve subsequently obtained in the normal manner. This time-consuming procedure was not followed in the present work.

## 2. Recovery

One overriding difficulty impedes every detailed analysis of DISA phenomena in AgMg: general recovery takes place in the same temperature range. In other words, the dislocation structure which provides the segregation sites for the solute atoms is itself not stable during the experiments reported. A clean analysis of DISA phenomena with a constant dislocation structure is therefore impossible here, unlike the case of steel in the studies of Conrad and Shoenck.<sup>(45)</sup>

For example, the incidence of inverse grain size dependence of flow stress at unusually low and intermediate temperatures is presumably a result of interference from a concomitant recovery process, although an exact mechanism cannot be deduced at this time. Again, drawing from experience with nominally pure metals, it is usually observed that transition temperatures, pinning phenomena, etc., are associated with an increased dependence of the yield stress on temperature. Such a contrast is not seen in AgMg both because of the strong temperature dependence of the concurrent recovery and because of an unusually high dependence of yield stress on temperature in the low-temperature region.

### 3. Mechanisms

If excess silver and/or magnesium atoms can act as the segregating species, then the results described above are not surprising. On the other hand, coincidence of recovery and DISA effects on the temperature scale does not prove that the ultimate rate controlling process is the same in the two cases. There is, in fact, some evidence that the processes are not the same. The activation energy deduced for the lower yield flow stress is 28 kcal for silver-rich and 40 kcal for magnesium-rich material, whereas the  $\text{Ag}^{110}$  diffusion activation energies are more than 40 kcal on the silver-rich side of stoichiometry and about 36 kcal on the magnesium-rich side. The 28 kcal energy must be (a) referred to the motion of some atomic species other than the component metals silver and magnesium, or (b) attributed to movement of the component species by some (short-circuiting) path other than volume diffusion, or (c) dismissed as a fictitious value resulting from the concurrent operation of two or more processes.

Another problem is concerned with the identification of the segregating species. According to Frank, (62) in order that dislocations be immobilized it should be necessary to pin both edges and screws. Spherical distortions such as are imparted by substituted atoms or vacancies can interact with the hydrostatic component of the stress field of an edge dislocation and so pin it, (5) but screw dislocations require an interaction between their own shear stress and that of a nonsymmetric distortion for pinning to occur. (6) Hence, simple monatomic point defects associated with compositional deviations from stoichiometry can account only for pinning of edge dislocations. Therefore, it must be assumed either that such defects are paired or that a nonsymmetrical distortion is provided by some extraneous impurity. The observed approximate independence of the pinning phenomena on composition might be significant in this regard but the relatively small concentrations estimated to be required for pinning (<0.1 per cent) make a decisive conclusion impossible.

#### C. The High-Temperature Region

The effects of composition and temperature on the flow stress in the high-temperature region are in accord with the earlier observations on the indentation hardness. (9) Whereas at the lower temperatures defects are a major impediment to slip and thereby raise the flow stress, in the high-temperature range they lower the flow stress except when present in very small concentrations. It is presumed that at high temperatures the defects influence the flow stress by an enhancement of diffusion rates which are assumed to be the rate-controlling process at these temperatures. Further support for this presumption will be given below. The local minima near stoichiometry in the flow stress isotherms are taken to be indicative of the greater effect of small defect concentrations on slip than on diffusion. Solution enhanced diffusion rates may also be a contributing factor in the solution softening effects noted in high-temperature deformation studies of terminal solid solutions, e. g.,  $\alpha$ -brass, (63) and iron-carbon. (64)

The analyses of Fig. 29 of temperature and strain rate effects demonstrated that flow in the high-temperature range is an activated process. Values of the activation energy  $E$  from Fig. 29 are plotted against composition in Fig. 33. Also shown in Fig. 33 are activation energies for  $\text{Ag}^{110}$  diffusion<sup>(12)</sup> and for grain growth.\* While the activation energies are composition dependent, there is no discontinuity at stoichiometry as was observed in the intermediate temperature region where DISA effects occur. The approximate numerical agreement of the deformation energies with the activation energy for diffusion of  $\text{Ag}^{110}$  and for grain growth may be only fortuitous since it is not known whether silver or magnesium is the faster moving species. Both deformation and grain growth would be expected to be controlled by the slower moving species. The decreasing trend of  $\text{Ag}^{110}$  diffusion activation energy with increasing magnesium content is, however, probably indicative of a general loosening of the lattice, an observation which is also supported by the magnesium activity measurements of Kachi.<sup>(32)</sup> Creep studies of  $\text{AgMg}$  in this temperature range would be more directly interpretable.

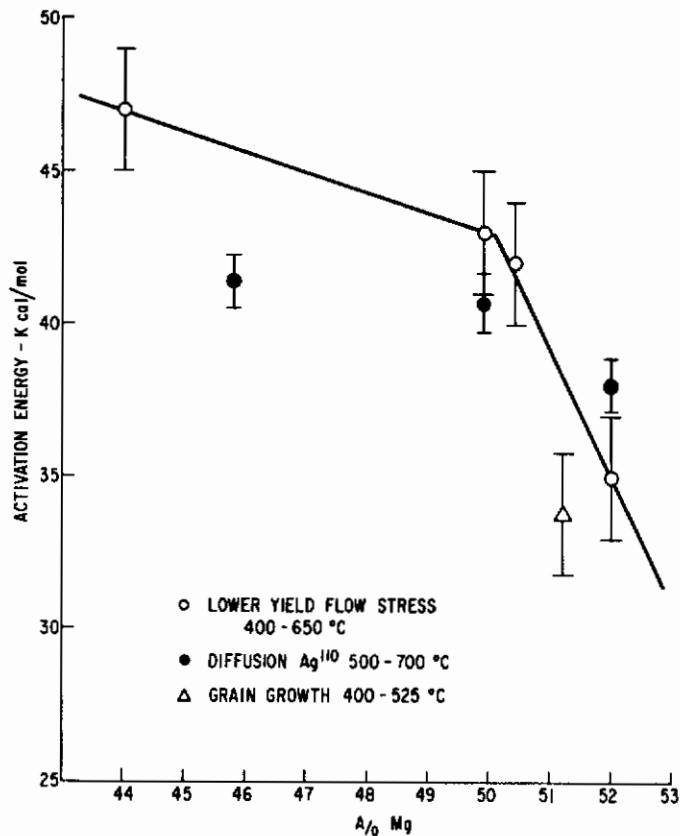


Fig. 33 Activation energies for various high-temperature rate processes as a function of temperature.

\*Data obtained by the authors in an auxiliary study.

## V. STUDIES OF OTHER COMPOUNDS

While the majority of the quantitative studies in this research have been performed on the compound AgMg, some exploratory and qualitative investigations have been carried out using other compounds. These studies will now be reported.

### A. NiAl

This intermetallic compound was chosen for study in conjunction with the work on the compound AgMg not only because it is isomorphous with AgMg--and thus lends itself to attempts at generalizations of behaviors observed in the experimentally more tractable AgMg--but also because its high melting point (1650°C) and oxidation resistance make it a promising practical material if a solution to the ductility problem is found.

During the first year's work, as described in previous reports under this contract, (2, 4) techniques for casting and extruding NiAl were explored, and extrusion to 1/2-inch-diameter rod and to 0.2-inch-thick strip was accomplished. Studies of the effects of the extrusion process and of subsequent heat treatments on the grain structure were also carried out. (4)

Although no mechanical tests have been performed on NiAl, specimens suitable for tensile testing have been produced. The direct extrusion of NiAl to wire test specimens, as has been accomplished for Bi<sub>2</sub>Tl and AgMg, is precluded for the higher melting NiAl by virtue of practical limitations of heat loss and extrusion mechanics. It has been pointed out in previous reports under this contract that NiAl can be extruded only at temperatures somewhat above 1000°C, and successful extrusion can be accomplished only if the reduction in area of the cross section exceeds about 12 to 1. These combined requirements, together with the pressure limitations of the press and heat loss from the billet during the process, permit as a lower limit the extrusion of a 2-inch-diameter billet to 1/2-inch-diameter rod.

Since a product of the order of 1/4-inch diameter is considered to be the largest size suitable for tensile specimen stock, it was necessary to modify the extrusion procedure in such a way as to circumvent these limitations. This modification was in the form of a multiple-hole die, designed to produce simultaneously five 1/4-inch-diameter rods from a 2-inch-diameter billet. Such a modification gives a total reduction in area suitable for successful extrusion with pressure requirements within the capacity of the press, while at the same time it avoids the problem of excessive cooling of the billet during the extrusion process. By this method, several ingots have been extruded to 1/4-inch-diameter rod. Sections of such extruded rod have been successfully ground to a shape suitable for tensile testing with no evidence of macro- or micro-cracking being found in a dye check test.



Because of the possibility that the grinding of extruded rods to suitable test specimen shape might have introduced surface defects having deleterious effects on the mechanical properties, it was thought advisable to carry out, at least during the early stages of the program, a parallel alternative effort for the production of suitable test specimens. The technique chosen for this purpose was the hot-rolling of extruded strip to sheet stock which would be tested directly. Extruded strip 0.2 inch thick by 1 inch wide was hot-rolled to a thickness of about 0.075 inch while encased in a stainless steel jacket. Such sheet was generally sound but exhibited an appreciable amount of surface cracking. The success of the multiple-hole die extrusion technique for tensile specimens, however, lessened the importance of the hot-rolled strip approach, and no further work has been done to improve the hot-rolled surface.

## B. Bi<sub>2</sub>Tl

The initial work under this contract was carried out on the hexagonal compound Bi<sub>2</sub>Tl, as has been reported previously.<sup>(2,4)</sup> Chosen primarily because of its low melting point and ease in handling, this material was used to establish processing and testing techniques which were later applied to the more difficult materials AgMg and NiAl.

A preliminary study of the effects of temperature and strain rate on the flow stress and ductility of this material was made in order to provide a basis for subsequent testing of AgMg. A detailed study was not made, however, since this material was found to have a recrystallization temperature below room temperature.

## C. TiAl

TiAl ingots, 4 inches in diameter, were prepared by the arc-melting process but no attempt has yet been made to extrude them.

## D. LaPb<sub>3</sub>

The success of the processing and testing techniques developed for AgMg in enabling the efficient and extensive documentation of tensile properties prompted a search for another compound to which these techniques could be directly translated without further development. Objectives of work on a new compound were not only to assess the generality of certain significant observations made on AgMg but also to extend the documentation of the mechanical behaviors of intermetallics by examining a compound with a different crystal structure. A survey was made, therefore, of compounds similar to AgMg with respect to congruency of melting, temperature of melting, retention of order to the melting point, and structural simplicity, but differing from AgMg

with respect to the specific crystal structure. The ordered face-centered cubic compound  $\text{LaPb}_3$  (mp is  $\sim 1000^\circ\text{C}$ ) was chosen for this study, and several compositions on either side of stoichiometry were cast into extrusion billet shape. No attempt has yet been made to extrude any of these billets, however, since none of the compositions cast could be made single phase by homogenization treatments. It would appear that the concentration range over which  $\text{LaPb}_3$  exists as a single phase may be so limited as to preclude preparation of single-phase material in bulk samples.

## VI. SUMMARY AND CONCLUSIONS

The first extensive documentation of the mechanical behaviors of an ordered intermetallic compound (AgMg) has been completed and is reported herein. Exploratory studies on several other compounds indicate that with some modifications the processing techniques and experimental approach used for AgMg can be successfully applied.

Analyses of tensile experiments on AgMg, together with the results of certain auxiliary experiments permit distinction of three regimes of deformation behavior:

1. Low temperatures and moderate strain rates where deformation is primarily by slip
2. Intermediate temperatures and low to moderate strain rates where deformation behavior is dominated by dislocation interactions with solute atoms
3. High temperatures and low strain rates where deformation is primarily by diffusion controlled processes.

Further specific conclusions derived from the experiments on AgMg are as follows:

### Low-Temperature Region

1. Solid solution strengthening resulting from lattice distortion can be expressed analytically by  $\sigma = K\Delta^s$ . The observation that  $s$  is a fractional power is not explained by present-day theories.
2. Stress-strain data conform to the relation  $\sigma = K\epsilon^m$ .

3. Highly ordered structures (near stoichiometric composition) work harden 3 to 4 times faster than highly defective structures, although this effect disappears at temperatures greater than about 200°C ( $\sim 0.4 T_{mp}$ ).

4. The strain hardening coefficient  $m$  and the flow stress  $\sigma$  are complementary and can be related by an empirical formula

$$\log m = K - K' \log \sigma.$$

5. The slip systems are  $\{321\}$ ,  $\{211\}$ ,  $\{110\}$  with  $\langle 111 \rangle$ .

6. Prestrain at high temperatures and low strain rates has a beneficial effect on subsequent deformability at low temperatures and/or at high strain rates.

7. Fracture is normally intercrystalline, but at low temperatures and high strain rates (211) cleavage occurs.

### Intermediate Temperature Region

8. Deformation is dominated by dislocation-solute atom interactions which give rise to several effects: deviation from monotonic stress-temperature curves, maxima in the change of strain rate sensitivity with temperature, minima in the temperature dependence of the strain hardening coefficient, pronounced yield points, inverse yield points in rate change tests, serrated stress-strain curves, strain aging, and strong stress relaxation effects.

9. The temperature dependence of the stress approximates a  $\sigma - 1/T$  law.

10. At constant temperature stress and strain rate are related by an exponential function

$$\log \sigma = K + K' \log \dot{\epsilon}$$

11. The deformation process is an activated process with an apparent activation energy of  $\sim 28$  kcal for Ag-rich and  $\sim 40$  kcal for Mg-rich material.

### High-Temperature Region

12. Lattice defects resulting from markedly off-stoichiometric composition tend to lower the flow stress; this presumably results from the enhancement of diffusion in a diffusion-controlled deformation process.

13. The variation with composition of the activation energy for deformation correlates with the variation with composition of the energy for Ag diffusion in AgMg.

## VII. RECOMMENDATIONS

The experimental program reported herein not only has extended considerably the understanding of the mechanical behavior of intermetallic compounds, but also has made recognizable some gaps in this understanding. The recognition of such gaps makes it possible to describe some of the needs for further work in this area.

An obvious need is the establishment of the generality with respect to other types of intermetallic compounds of the principles and effects found for AgMg. The extent of such generality could be clarified by an exploration of one or more other compounds in a manner similar to that reported herein. In addition to such a rather broad exploration, other more specific suggestions can be made concerning future investigations:

1. An extension of the studies of the effects of pre-strain on ductility.
2. A detailed study of the nature of grain boundaries and adjacent regions, including considerations of
  - (a) Composition
  - (b) Mechanical properties
  - (c) Fractographic studies of grain boundary surfaces.
3. Single-crystal studies which would eliminate grain boundary effects from the several phenomena identified herein.
4. An extension of the studies of the effects of ternary additions in order to establish the mechanism of their effect on ductility.
5. Experiments aimed at the identification of both the atomic species and the mechanisms underlying the observed effects of dislocation interaction with solute atoms.
6. Measurement of the diffusion coefficients of Mg in AgMg, either directly or indirectly.

## VIII. OTHER ACTIVITIES

During the past year the proceedings of the 1959 International Symposium on "The Mechanical Properties of Intermetallic Compounds" were published by John Wiley and Sons, Inc., under the editorship of one of the authors (JHW).

# *Contrails*

This work included contributions by each of the authors: a review article (JHW) and a research paper (DLW), the latter based on work supported by this contract.

In March 1960 one of the authors (DLW) attended and presented a paper, "Some Aspects of the Tensile Behavior of the Intermetallic Compound AgMg," at a Conference on Mechanical Properties of Engineering Ceramics at North Carolina State College. The technical papers of this conference will appear at a later date in book form.

## REFERENCES

1. J. H. Westbrook, "Mechanical Properties of Intermetallic Compounds--A Review of the Literature," from the Symposium Mechanical Properties of Intermetallic Compounds, J. H. Westbrook, ed., John Wiley and Sons, Inc., New York (1960), p. 1.
2. D. L. Wood, "Extrusion of Intermetallic Compounds," from the Symposium Mechanical Properties of Intermetallic Compounds, J. H. Westbrook, ed., John Wiley and Sons, Inc., New York (1960), p. 161.
3. D. L. Wood, "Some Aspects of the Tensile Behavior of the Intermetallic Compound AgMg," from Mechanical Properties of Engineering Ceramics--A Symposium, North Carolina State College, 1960 (to be published). See also GE Research Lab. Rept. No. 60-GC-109.
4. D. L. Wood and J. H. Westbrook, "Effect of Basic Physical Parameters on Engineering Properties of Intermetallic Compounds," WADD Tech. Rept. No. 60-184, August 1960.
5. A. H. Cottrell and B. A. Bilby, "Dislocation Theory of Yielding and Strain Aging in Iron," Proc. Phys. Soc., A62, 49 (1949).
6. A. W. Cochardt, G. Schoeck, and H. Wiedersich, "Interaction Between Dislocations and Interstitial Atoms in Body-Centered Cubic Metals," Acta Met., 3, 533 (1955).
7. W. G. Johnston and J. J. Gilman, "Dislocation Velocities, Dislocation Densities, and Plastic Flow in Lithium Fluoride Crystals," J. Appl. Phys., 30, 129 (1959).
8. A. H. Cottrell and M. A. Jaswon, "Distribution of Solute Atoms Round a Slow Dislocation," Proc. Phys. Soc., A199, 104 (1949).
9. J. H. Westbrook, "Defect Structure and the Temperature Dependence of Hardness of an Intermetallic Compound," J. Electrochem. Soc., 104, 369 (1957).
10. E. Parker, "Principles of Solution Hardening," Relation of Properties to Microstructure, ASM, Cleveland (1954), p. 30
11. N. V. Ageev and V. G. Kuznetsov, "X-Ray Study of Alloys of Mg and Ag," Bull. acad. sci. URSS, 289 (1937).

# Contrails

12. W. C. Hagel and J. H. Westbrook, "Silver Diffusion in the Intermetallic Compound AgMg" (unpublished).
13. R. P. Carreker, "Tensile Deformation of Silver as a Function of Temperature, Strain Rate, and Grain Size," Trans. AIME, 209, 112 (1957).
14. J. W. Pugh, "Temperature Dependence of the Tensile Properties of Vanadium," Trans. AIME, 209, 1243 (1957).
15. R. P. Carreker and R. W. Guard, "Tensile Deformation of Molybdenum as a Function of Temperature and Strain Rate," Trans. AIME, 206, 178 (1956).
16. J. W. Pugh, "Temperature Dependence of the Tensile Properties of Tantalum," Trans. ASM, 48, 677 (1956).
17. J. H. Bechtold, "Strain Rate Effects in Tungsten," Trans. AIME, 206, 142 (1956).
18. G. Sachs and J. Weerts, "Atomic Ordering and Property Investigations on the Alloy AuCu<sub>3</sub>," Z. Physik, 67, 507 (1931).
19. J. H. Hollomon, "Tensile Deformation," Trans. AIME, 162, 268 (1945).
20. W. A. Rachinger and A. H. Cottrell, "Slip in Crystals of the Cesium Chloride Type," Acta Met., 4, 1 (1956).
21. G. W. Ardley and A. H. Cottrell, "Yield Points in Brass Crystals," Proc. Roy. Soc., A219, 328 (1953).
22. C. S. Barrett, Structure of Metals, McGraw-Hill Book Co., Inc., New York (1952), pp. 337, 379, 386.
23. R. W. Guard and A. M. Turkalo, "Fractographic Studies in NiAl and Ni<sub>3</sub>Al," from the Symposium Mechanical Properties of Intermetallic Compounds, J. H. Westbrook, ed., John Wiley and Sons, Inc., New York (1960), p. 141.
24. J. R. Low, "A Review of the Microstructural Aspects of Cleavage Fracture," from Fracture, Tech. Press and John Wiley and Sons, Inc., New York (1959), p. 68.
25. J. D. Lubahn, "Strain Aging Effects," Trans. ASM, 44, 643 (1952).

26. I. Kramer and R. Maddin, "Delay Time for the Initiation of Slip in Metal Single Crystals," Trans. AIME, 194, 197 (1952).
27. J. W. Allen, "Mechanical Properties of Indium Antimonide," Phil. Mag., 2, 1475 (1957).
28. J. W. Allen, "On the Delay Time in Plastic Flow of Indium Antimonide," Phil. Mag., 3, 1297 (1959).
29. R. H. Baskey, "Research on the Delay Time Study of Metal Single Crystals," Office of Naval Research (July 1958), 70 pp.
30. J. C. Fisher, "Application of Cottrell's Theory of Yielding to Delayed Yield in Steel," Trans. ASM, 47, 451 (1955).
31. R. L. Fleischer, "Long-Range Pinning of Dislocations by Atomic Defects," GE Research Lab. Rept. No. 61-RL-2603 M (January 1961).
32. S. Kachi, "Thermodynamic Properties of  $\alpha$  and  $\beta$  Silver-Magnesium Alloys," Sci. Repts. Res. Inst. Tohoku Imp. Univ., A7, 351 (1955).
33. W. Trzebiatowski and J. Terpilowski, "Thermodynamic Properties of the Silver-Zinc System and the Related  $\beta$  AgMg Phase," Bull. acad. polon. sci., 3, 391 (1955).
34. Y. Shibuya, "The Variation of Young's Modulus of Binary Body-Centered Cubic Alloys Caused by the Formation of a Superlattice," Tohoku Univ. Sci. Repts. Res. Inst., A1, 161 (1949).
35. G. W. Ardley, "On the Effect of Ordering Upon the Strength of  $\text{Cu}_3\text{Au}$ ," Acta Met., 3, 525 (1955).
36. N. Brown, "The Yield Point of a Superlattice," Phil. Mag., 4, 693 (1959).
37. D. Tabor, "A Simple Theory of Static and Dynamic Hardness," Proc. Roy. Soc., A192, 247 (1948).
38. D. Tabor, The Hardness of Metals, Oxford Press (1951).
39. E. D. Levine, W. F. Sheely, and R. R. Nash, "Solid Solution Strengthening of Magnesium Single Crystals at Room Temperature," Trans. AIME, 215, 521 (1959).



# Contrails

40. D. Hardie and R. N. Parkins, "Solid Solution Hardening of Aluminum and Magnesium," J. Inst. Metals, 85, 449 (1956-7).
41. A. H. Cottrell, "Interactions of Dislocations and Solute Atoms," Relation of Properties to Microstructure, ASM (1953), p. 151.
42. H. J. Logie, "The Yield Strength of Partly Ordered F. C. C. Structures," Acta Met., 5, 106 (1957).
43. C. S. Barrett, "Effects of Temperature on the Deformation of Beta Brass," Trans. AIME, 200, 1003 (1954).
44. W. L. Bragg, "The Structure of a Cold Worked Metal," Proc. Phys. Soc., 52, 105 (1940).
45. H. Conrad and G. Schoeck, "Cottrell Locking and the Flow Stress in Iron," Acta Met., 8, 791 (1960).
46. P. A. Flinn, "Theory of Deformation in Superlattices," Trans. AIME, 218, 145 (1960).
47. N. Brown, "The Interaction Between Dislocations and the Superlattice," Mechanical Properties of Intermetallic Compounds, J. H. Westbrook, ed., John Wiley and Sons, Inc., New York (1960), p. 177.
48. G. Schoeck and A. Seeger, Defects in Crystalline Solids, Bristol, 341 (1955).
49. G. Sachs, "Effect of Strain on Fracture," Fracturing of Metals, ASM, Cleveland (1948).
50. E. J. Ripling and W. M. Baldwin, Jr., "Rheotropic Embrittlement of Steel," Trans. ASM, 43, 778 (1951).
51. E. J. Ripling and W. M. Baldwin, Jr., "Overcoming Rheotropic Brittleness: Precompression versus Pretension," Trans. ASM, 44, 1047 (1952).
52. E. J. Ripling, "Strain Aging Behavior of Rheotropically Embrittled Steel," Trans. ASM, 46, 184 (1954).
53. E. J. Ripling, "Rheotropic Embrittlement," Bull. ASTM (December 1952), p. 37.
54. E. J. Ripling and W. M. Baldwin, Jr., "Rheotropic Brittleness--General Behaviors," Proc. ASTM, 51, 1023 (1951).

55. P. E. Wretblad, "Manufacture of Tungsten Metal," in Powder Metallurgy, J. Wulff, ed., ASM, Cleveland (1941).
56. Z. Jeffries and R. S. Archer, "Effect of Temperature Pressure and Structure on Mechanical Properties of Metal," Chem. Met. Eng., 27, 747 (1922).
57. A. W. Magnusson and W. M. Baldwin, "Low Temperature Brittleness," J. Mech. Phys. Solids, 5, 172 (1957).
58. R. Bakish and W. D. Robertson, "Structure Dependent Chemical Activity of Polycrystalline  $Cu_3Au$ --Experiments Relating to the Mechanism of Stress-Corrosion Cracking of Homogenous Solid Solutions," Trans. AIME, 206, 1003 (1954).
59. M. Herman, private communication to Brown; see Ref. 47.
60. A. H. Cottrell, "A Note on the Portevin-LeChatelier Effect," Phil. Mag., 44, 829 (1953).
61. W. G. Johnston, private communication.
62. F. C. Frank; see A. H. Cottrell, "The Yield Point in Single Crystal and Polycrystalline Metals," in Plastic Deformation of Crystalline Solids, Pittsburgh (1950), p. 60.
63. S. I. Gubkin and P. A. Zacharov, "Mechanical Properties of the System Copper-Zinc," Izvest. Akad. Nauk SSSR, 41 (1937).
64. K. A. Osipov and E. M. Miroshkina, "Hardness of the Gamma Solid Solution in the Iron-Carbon System at High Temperatures," Doklady Akad. Nauk USSR, 94, 1065 (1954); Brutcher Transl. No. 3332.

## APPENDIX

SUMMARY OF TENSILE STRESS DATA

TABLE III

Intended and Analyzed Compositions of AgMg Compounds

Intended Composition (wt % Mg)	Analyzed Composition	
	(wt % Mg)	(at. % Mg)
15.0	15.0 ± 0.05	43.9 ± 0.09
16.0	16.0	45.8
16.0	16.2	46.2
17.2	17.2	48.0
17.8	17.8	49.0
18.0	18.1	49.5
18.3	18.3	49.8
18.6	18.6	50.3
19.0	19.1	51.2
19.3	19.3	51.5
19.6	19.6	52.0
21.0	21.1 ± 0.05	54.3 ± 0.08
18.2 + 1.0 W/o Zn	18.2 + 1.0 W/o Zn	49.4 + 1.0 A/o Zn
18.1 + 1.8 W/o Sn	18.1 + 1.7 W/o Sn	49.5 + 1.0 A/o Sn

TABLE IV

Stress ( $L/A_0$ ) at 0.2 Per Cent Offset for Various Temperatures and Strain Rates for Silver-rich Compounds; Given in 1000 psi for Material of Grain Diameter  $\sim 1.7 \times 10^{-3}$  cm (as-extruded)

$\dot{\epsilon}$ %/min <sup>-1</sup>	Atomic Per Cent Magnesium															
	43.9		45.9		46.2		48.0		48.0		48.5		49.4		49.5	
T(°C)	0.5	0.5	5.0	5.0	20.0	30.0	0.5	0.5	0.5	5.0	20.0	50.0	0.5	0.5	0.5	0.5
25	45.6	40.0	38.8	41.0	42.2	43.7	33.6	28.8	22.6	22.0	21.2	22.5	--	--	--	--
	64.7*	60.8*	--	--	--	--	55.2*	54.0*	48.8*	--	--	--	--	--	--	--
100	40.8	35.1	35.5	--	--	--	28.8	26.7	21.0	--	--	--	27.6	--	--	--
	58.6*	--	--	--	--	--	--	38.2*	--	--	--	--	--	--	--	--
150	37.1	31.6	--	--	--	--	28.0	22.0	19.0	--	--	--	--	--	--	--
175	--	--	24.8	30.8	33.0	34.0	--	--	15.4	17.9	19.1	20.2	--	--	--	--
200	22.8	20.4	19.5	26.9	30.3	32.7	17.9	14.8	11.8	15.5	17.6	19.1	22.2	--	--	25.6
225	--	--	15.0	21.4	25.9	29.8	--	--	8.40	12.5	15.3	17.6	--	--	--	--
250	--	--	12.0	18.3	21.9	26.5	--	--	7.15	10.0	13.1	15.0	--	--	--	--
270	--	--	10.1	--	--	--	--	--	6.00	--	--	--	--	--	--	--

NOTE: Underlined values in this and other tables indicate values of flow stress obtained in rate change tests in which the strain rate was increased after initial yielding at a lower strain rate.

\*Stress at 8 per cent elongation.

TABLE V

Stress ( $L/A_0$ ) at 0.2 Per Cent Offset for Various Temperatures and Strain Rates for Magnesium-rich Compounds; Given in 1000 psi for Material of Grain Diameter  $\sim 1.7 \times 10^{-3}$  cm (as-extruded)

$\dot{\epsilon}$ %/min <sup>-1</sup>	Atomic Per Cent Magnesium																
	50.3		51.2		51.5		52.0		54.3		54.3						
T(°C)	0.2	0.5	1.0	2.0	5.0	10.0	20.0	0.2	0.5	2.0	0.2	0.5	2.0	0.2	0.5	2.0	
200	19.2	20.6	23.5	22.7	26.0	--	--	33.2	--	25.6	31.8	--	29.2	35.5	--	--	--
225	12.5	15.0	19.0	--	18.7	22.0	--	27.3	--	18.1	21.2	26.8	20.6	24.3	30.9	20.2	24.0
250	9.00	10.8	13.9	12.8	14.6	15.7	18.0	20.6	25.2	13.8	16.2	19.8	14.6	17.3	22.5	13.0	15.7
270	7.60	8.90	11.1	--	11.3	--	16.2	--	9.9	1.0	3.0	16.2	11.6	14.3	18.0	--	11.5

TABLE VI

Stress ( $L/A_0$ ) at 0.2 Per Cent Offset for Various Temperatures and Strain Rates  
for Silver-rich Compounds; Given in 1000 psi for Material  
of Grain Diameter  $\sim 2.8 \times 10^{-3}$  cm (annealed at  $400^\circ\text{C}$ )

$\dot{\epsilon}$ % ( $\text{min}^{-1}$ )	Atomic Per Cent Magnesium								
	43.9		46.2			49.0		49.5	
	0.5	5.0	0.5	1.0	5.0	0.5	5.0	0.5	1.0
T( $^\circ\text{C}$ )									
25	46.4	<u>48.0</u>	--	--	--	31.2	<u>35.2</u>	--	--
100	46.0	<u>48.8</u>	--	--	--	25.6	<u>29.7</u>	--	--
150	38.4	<u>44.7</u>	--	--	--	23.2	<u>27.6</u>	--	--
175	30.8	<u>38.9</u>	--	--	--	18.5	<u>24.4</u>	--	--
200	24.0	<u>31.3</u>	--	--	--	14.1	<u>20.5</u>	--	--
225	18.2	<u>24.6</u>	--	--	--	10.6	<u>15.8</u>	--	--
250	14.4	<u>19.3</u>	--	--	--	7.60	<u>11.4</u>	--	--
270 (oil)	12.0	<u>16.0</u>	--	--	--	6.40	<u>9.60</u>	--	--
270 (A)	12.6	<u>16.5</u>	--	--	--	7.45	<u>11.2</u>	--	--
300	10.2	<u>13.3</u>	10.1	--	--	5.44	<u>7.68</u>	4.90	--
350	7.60	<u>9.94</u>	7.10	--	--	4.44	<u>5.92</u>	4.00	--
375	--	--	5.80	--	--	--	--	3.50	--
400	5.60	<u>7.70</u>	5.25	5.90	6.90	3.52	<u>4.63</u>	3.10	--
425	--	--	4.80	4.95	--	--	--	2.85	2.80
450	3.68	<u>5.60</u>	4.50	4.50	--	2.72	<u>3.52</u>	2.6	2.50

TABLE VII

Stress ( $L/A_0$ ) at 0.2 Per Cent Offset for Various Temperatures and Strain Rates for Magnesium-rich Compounds; Given in 1000 psi for Material of Grain Diameter  $\sim 2.8 \times 10^{-3}$  cm (annealed at  $400^\circ\text{C}$ )

$\dot{\epsilon} \rightarrow$ % ( $\text{min}^{-1}$ )	Atomic Per Cent Magnesium									
	50.3		51.2			51.5		54.3		
	0.5	5.0	0.5	1.0	5.0	0.5	5.0	0.5	1.0	5.0
T ( $^\circ\text{C}$ )										
175	24.5	--	--	--	--	--	--	--	--	--
200	19.7	<u>24.4</u>	26.2	28.5	<u>35.0</u>	--	--	--	--	--
225	15.2	<u>19.8</u>	20.2	22.2	<u>28.5</u>	--	--	--	--	--
250	11.2	<u>15.6</u>	14.6	16.8	<u>20.8</u>	16.8	<u>23.6</u>	--	--	--
270 (oil)	8.15	<u>11.9</u>	12.3	--	<u>17.4</u>	13.2	<u>18.6</u>	--	--	--
270 (A)	9.04	<u>13.0</u>	--	--	--	15.6	<u>19.8</u>	--	--	--
300	6.40	<u>9.30</u>	9.40	--	--	10.4	<u>14.4</u>	15.5	--	--
350	4.86	<u>6.86</u>	6.60	--	--	8.00	<u>10.3</u>	9.20	--	--
375	--	--	5.30	--	<u>8.60</u>	--	--	6.40	--	--
400	3.28	<u>4.47</u>	4.80	4.65	<u>6.00</u>	4.07	<u>6.68</u>	5.15	--	--
425	--	--	4.10	4.15	<u>5.40</u>	--	--	3.70	3.00	<u>4.80</u>
450	--	--	3.60	3.70	<u>4.90</u>	--	--	2.50	2.50	<u>3.90</u>

TABLE VIII

Stress ( $L/A_0$ ) at 0.2 Per Cent Offset for Various Test Temperatures;  
 Given in 1000 psi for Material of Grain Diameter  $\sim 6.4 \times 10^{-3}$  cm  
 (annealed at  $500^\circ\text{C}$ ), Strained at a Rate of 0.5 Per Cent ( $\text{min}^{-1}$ )

T( $^\circ\text{C}$ )	Atomic Per Cent Magnesium								
	<u>43.9</u>	<u>45.9</u>	<u>48.0</u>	<u>49.0</u>	<u>49.8</u>	<u>50.3</u>	<u>51.2</u>	<u>51.5</u>	<u>52.0</u>
-196	68.4	57.4	48.4	38.8	28.0	--	--	--	--
-75	54.4	47.2	38.0	28.0	20.4	--	--	--	--
25	44.5	41.1	32.4	24.3	17.1	--	--	--	--
75	43.1	39.2	30.8	23.2	14.8	--	--	--	--
100	41.7	37.5	30.5	23.2	14.4	--	--	--	--
125	--	36.3	28.5	22.0	14.4	--	--	--	--
140	--	--	28.8	--	--	--	--	--	--
150	36.7	34.6	26.6	20.9	12.8	--	--	--	--
160	--	--	27.2	--	--	--	--	--	--
175	--	--	24.8	--	--	21.2	--	--	--
190	--	--	22.4	--	--	--	--	--	--
200	23.5	21.2	17.0	14.0	9.35	18.5	--	--	--
215	--	--	14.8	--	--	--	--	--	--
225	--	--	13.6	--	--	--	--	--	--
250	15.0	13.7	10.5	8.50	4.80	12.6	--	17.2	20.2
300	9.05	8.80	6.30	5.45	3.28	6.65	10.2	10.6	11.8
400	5.75	5.27	3.87	2.83	2.18	3.08	3.90	4.25	4.30
500	2.56	2.80	2.36	1.96	1.62	1.68	2.04	1.92	1.65

TABLE IX

Stress ( $L/A_0$ ) at 8 Per Cent Elongation for Various Test Temperatures;  
 Given in 1000 psi for Material of Grain Diameter  $\sim 6.4 \times 10^{-3}$  cm  
 (annealed at  $500^\circ\text{C}$ ), Strained at a Rate of 0.5 Per Cent ( $\text{min}^{-1}$ )

T( $^\circ\text{C}$ )	Atomic Per Cent Magnesium								
	43.9	45.9	48.0	49.0	49.8	50.3	51.2	51.5	52.0
25	55.0	51.0	45.5	41.5	36.5	--	--	--	--
100	51.7	48.7	42.4	36.5	29.0	--	--	--	--
125	--	44.0	38.0	32.0	24.5	--	--	--	--
200	26.6	23.5	18.9	15.6	10.8	19.5	--	--	--
250	17.4	15.5	12.6	--	6.95	10.4	--	17.0	18.4
300	10.7	10.5	7.90	6.55	4.45	6.15	8.80	10.8	11.2
400	5.75	5.86	4.87	3.75	2.69	3.08	3.60	3.80	3.70
500	2.24	2.40	2.28	2.14	1.62	1.72	1.88	1.70	1.52



